Historical palaeohydrology and landscape resilience of a Mediterranean rambla (Castellón, NE Spain): Floods and people

M.J. Machado [a, *], A. Medialdea [b], M. Calle [a], M.T. Rico [c], Y. Sánchez-Moya [d, e], A. Sopeña [d], Benito [a]

[a] *Geology Department, National Museum of Natural Sciences -CSIC, Madrid, Spain*
[b] *Department of Geography, University of Sheffield, Winter Street, S10 2TN, Sheffield, UK*
[c] *Instituto Pirenaico de Ecología, CSIC, Zaragoza, Spain*
[d] *Geosciences Institute, CSIC-University Complutense of Madrid, Spain*
[e] *Department of Stratigraphy, University Complutense of Madrid, Spain*

A B S T R A C T

This paper provides a new methodological approach to analyse secular patterns of flooding (magnitude and frequency) from sedimentary evidence (palaeofloods), taking into account changes in channel geometry, and their links to historical environmental changes and the inherent social and demographic evolution within the catchment. A case study analysis was focused in Rambla de la Viuda (drainage area of 1500 km^2) whose stream flow is related to extreme rainfalls. A 500 years sedimentary archive was reconstructed from eight stratigraphic profiles comprising continuous sequences of slackwater flood deposits interbedded with episodic colluvial and edaphic horizons. Discharge estimates associated to sedimentary flood evidences were obtained from one-dimensional hydraulic modelling. The strati- graphic units were sampled to characterise their geochemical and paleobotanical (phytoliths) contents. Palaeoflood chronology was obtained from radiocarbon and luminescence (OSL) dating, supported by documentary data (written historical documents). A high frequency and high magnitude palaeoflood period took place during the 15th-middle 16th century, which seem to correlate in time with general wetter conditions. Three short-term environment stability conditions (land use and climatic) also made possible the development of three paleosols. The lowest flood magnitude and discharges in the sedi- mentary record was found between the mid-17th to mid-18th centuries, under prevailing drier envi- ronmental conditions. Episodic high magnitude flooding took place at late 18th century, correlating in time with palaeovegetation and geochemical evidences of important changes on land use (deforestation and grazing). Poorer developed soils were found at upper stratigraphic sequences (19th century) char- acterised by thick units of colluvium deposits, usually culminating sequences of short-lived continuous slackwater flood units. Despite of the potential human influence (land-use) on soil hydrology, the long- term behaviour of high magnitude floods (>1000 m^3 s^{-1}) has been stationary over the last 500 years.

Keywords: Palaeohydrology, Palaeofloods, Flood frequency analysis, Historical landcover

1. Introduction

In Mediterranean semiarid environments, floods are major drivers of geomorphological, hydrological, and ecological changes (Thornes et al., 2009). In Spain, large ephemeral gravel-bed rivers (known as *Ramblas*) are highly dependent on heavy rainfalls to generate streamflow, and only during large floods significant geo- morphologic changes take place (Mateu, 1988; Camarasa and Segura, 2001). These *ramblas* are relatively short in length (<100 km), draining small catchments (several hundred km^2) and present a steep slope due to their geomorphological emplacement within the mountain ranges that run parallel to the coast. These physiographic settings are highly favourable to generate flash floods transporting large volumes of sediment load (López-Bermúdez et al., 2002). A number of authors have recognised the role of these short-lived floods in maintaining the functionality of ephemeral fluvial landscapes and riparian ecosystems (Friedman and Lee, 2002), and their contribution to recharge alluvial aqui- fers through transmission losses (e.g. Shannon et al., 2002; Morin

* Corresponding author.
E-mail address: machado@mncn.csic.es (M.J. Machado).

et al., 2009; Dahan et al., 2008). Moreover, floods are of great significance to regional and local human activities (e.g. irrigated orchards and urban planning) and knowledge of them is critical when planning the design of infrastructures (dams, spillways, bridges). Dam construction for irrigation purposes has a long history in the region, earliest dated at 14th century (López Gómez, 1987), but spillway capacity and dam safety design frequently lack of adequate knowledge about the upper limit of extreme floods needed for risk analysis. A common problem to understand the flood hydrology of Mediterranean ephemeral rivers is the scarcity of hydrological data in terms of its spatial and temporal distribution. Large torrential events are difficult to monitor and it is frequent that where the record do exist, the data are partial (gauge instruments are frequently destroyed or flooded) and limited to few decades (Schick, 1988). Palaeoflood hydrology has contributed to extend the record of large floods back in time from centuries to millennia timeframes (Baker, 1987, 2008). Palaeoflood studies in bedrock rivers are typically based on stratigraphic descriptions of slackwater flood sediments deposited during high flood stage at high elevation marginal zones from which robust discharge estimates can be obtained based on hydraulic modelling (Benito and O'Connor, 2013).

Studies based on palaeoflood records from Europe (Benito et al., 2003a,b; Thorndycraft and Benito, 2006), Middle East (Greenbaum et al., 2000), Africa (Zawada, 2000; Benito et al., 2011; Grodek et al., 2013; Greenbaum et al., 2014), India (Kale, 2007), China (Huang et al., 2011; Zhang et al., 2013), New Zealand (Macklin et al., 2012), and the United States USA (Ely et al., 1993) have demonstrated the occurrence of temporal concentrations of floods (flood-rich periods) in response to centennial-scale hydroclimatic changes. These studies prove that rivers respond immediately to climate variations through changes in flooding regime linked to abrupt shifts in atmospheric circulation (Knox, 1983; Benito et al., 2015a,b). However, over the last millennia, an additional source of uncertainty is how climate variability and a long history of land-use changes have affected the frequency and magnitude of large floods (Benito et al., 2010; Rodriguez-Lloveras et al., 2015). Land-use and land-cover changes have been critical in terms of regional driving and/or amplifying mechanisms modifying the flood hydrology, sediment production and sediment loads and, therefore, the river morphodynamics (e.g. Gregory et al., 2006). The understanding of hydrological response to environmental history may provide new insight into the assessment of changes in the flood patterns to anthropogenic global change (Kundzewicz et al., 2013).

This paper aims to determine the way in which extreme events may be changing both in frequency and intensity as a result of climate variability and of human influences (land-use) on soil hydrology. The starting hypothesis is that when flood frequency recorded in slackwater flood deposits reflects changes in climate conditions, contemporaneous changes in in sedimentological and biogeochemical characteristics may be linked to environmental changes at a basin scale. The case study for testing this hypothesis is Rambla de la Viuda, one of the largest ephemeral rivers in the Valencia region, eastern Spain. The Rambla's landscape shows ubiquitous crop terraces and afforested areas which provide evidence of a long environmental history of land-use changes. The biomineral and geochemical content of slackwater flood sediments provide signatures of specific environmental conditions at the flood time to enable interpretation of these environmental changes. The specific objectives are: (1) extend the record of the largest floods both in terms of chronology and magnitudes, (2) determine how the flood hydrology of a river responds to climate variability over time; (3) appraise the importance of land-use on the magnitude of present and past recorded events; (4) determination of the maximum limit of flood magnitude and non-exceedences as a check of the maximum floods estimated for this *rambla*, (5) assess the adequacy of the design of engineering infrastructures such as dams, and (6) enhance societal perception of floods, as the physical evidence of past extreme floods is preferable to statistical probabilities such as the 1 in 100 year flood.

2. Study area

Rambla de la Viuda, located in eastern Spain (Castellón Province), is a Mediterranean ephemeral river of ca 36 km in length and 1500 km^2 of catchment surface (Fig. 1). Rambla de la Viuda middle fork is composed of two main tributaries: Montlleó River and Rambla Carbonera. Their headwaters are located at the Iberian Range Mountains at 1250–1720 m a.s.l. giving rise to high average channel slope and high sediment load during torrential events. The catchment geology is dominated by Cretaceous and Jurassic limestones and marls of the eastern sector of the Iberian mountain chain affected by the Alpine tectonics reactivated during the Neogene that developed a sequence of horst and grabens running parallel to the coast (NNW-SSE; Simón et al., 2013). These grabens were filled by Neogene and Quaternary gravelly deposits which provide an important source of gravels to the present fluvial system. The Rambla de la Viuda runs north-south parallel to one of these Neogene basins (Albocasser-Rambla de la Viuda graben) and cuts through its southern border. In this lower reach, downstream of our study reach, the Rambla de la Viuda channel has incised into its former Pleistocene alluvial fan deposits where it joins the Millars River to find its way to the Mediterranean Sea.

In terms of climate, the mean annual precipitation ranges between 500 and 650 mm (Mateu, 1974). The region is affected by: (a) autumnal rains (September to November) giving the highest monthly precipitation records; and (b) frontal systems due to Atlantic zonal flow during winter (December to January) and spring (March–May), the latter responsible for the area secondary rainfall maximum. The hydrological regime is characterised by short-lived flows with an average of 2–3 events per year (rainfall >70 mm; Segura, 1990), producing stream flow only during ca 31 days per year (Camarasa and Segura, 2001). There is a good correlation between rainfall and runoff, although runoff coefficients are low (0.7%–17%) due to high transmission losses along the river course (Camarasa and Segura, 2001). Large floods are an important component of this irregular hydrological regime, giving up to 80% of annual runoff volume in a single event (Segura and Camarasa, 1996). The most intense rainfall conditions leading to extreme floods are associated to mesoscale convective systems (MCSs) (Llasat and Puigcerver, 1990) fed by moisture born in the Mediterranean and enhanced by the orographic effect of the mountain ranges near the coast. For instance, the rainfall episode of October 16th, 1962, rainfall intensity of ca. 300 mm in 24 h that, together with the steep gradients in the catchment, resulted in severe flash flooding with a peak discharge estimated in 1500 $m^3 s^{-1}$ at the Maria Cristina reservoir, that spilled over the dam wall with a depth of 0.7 m. The Maria Cristina dam located in the lower part of the catchment was built in 1925 with a capacity of 20 millions of m^3, and a spillway design to drain up to 600 $m^3 s^{-1}$. Similar large floods overflowing the dam wall occurred in 1920 (during dam construction works), 1962, 1969 and 2000. Currently, it is proposed the hydraulic design of a labyrinth spillway to drain a design flood between 3073 $m^3 s^{-1}$ and 2855 $m^3 s^{-1}$ (flood of 1000-yr occurrence interval) (Cordero Page et al., 2007). Daily water storage balance from this reservoir provides the longest hydrological record of the *rambla*, with available data since October 1959, and since January 2007 at 5-min intervals. The fluvial geomorphic activity is concentrated during the flood episodes during which a high

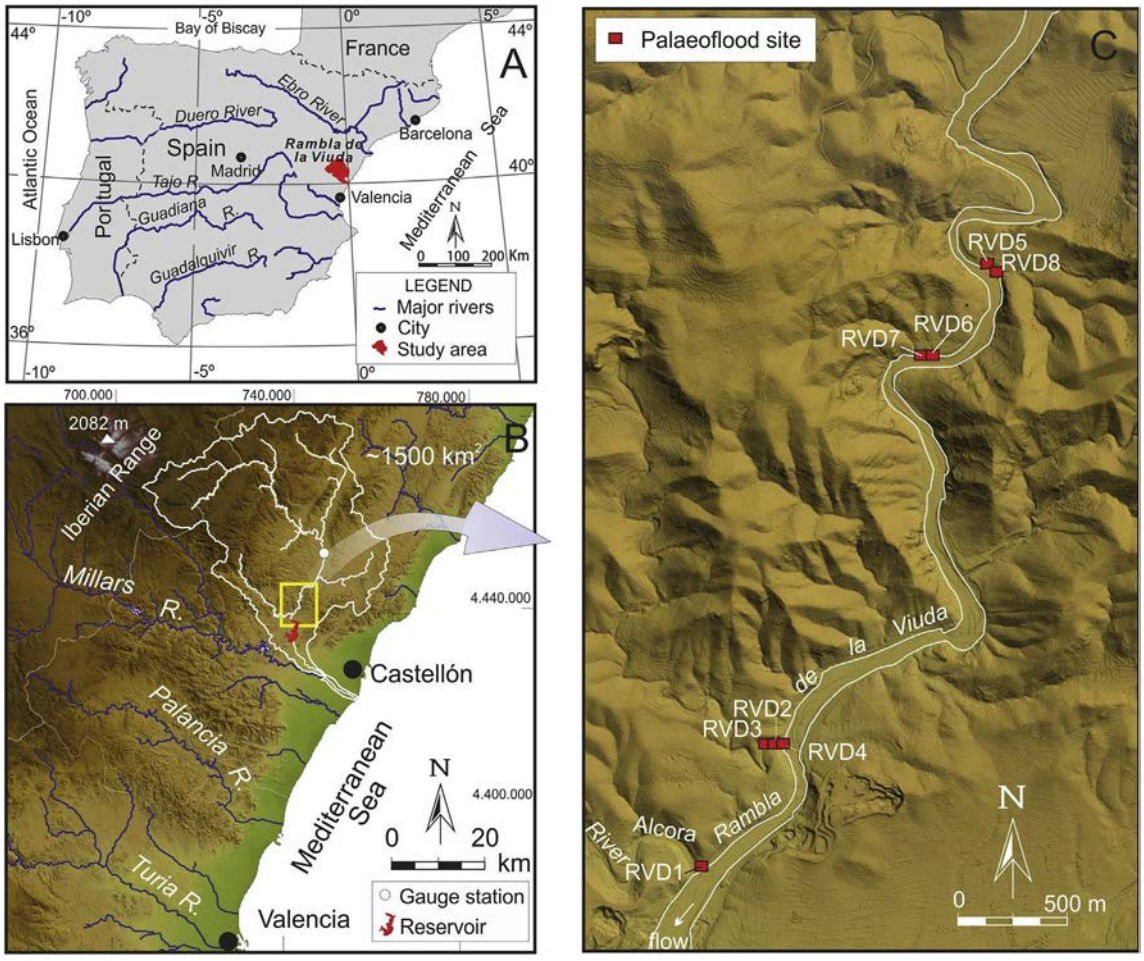

Fig. 1. A: The Rambla de la Viuda in the Iberian Peninsula. B: Rambla de la Viuda catchment in eastern Spain, and its junction with the Millars River ca 8 km before reaching the Mediterranean Sea. In the basin is shown the Montlleò river (west fork), the Carbonera Stream (east fork) together with the location of the studied reach, the SAIH gauge station (Vall d'Alba) and the Maria Cristina reservoir. C: Digital terrain model of the studied reach showing the river entrenchment on Cretacious limestones and Plio-Pleistocene conglomerates, and the location of the flood deposits stratigraphic profiles.

amount of sediment is transported towards the Maria Cristina reservoir (Mateu, 1975).

The palaeoflood study was focussed on a reach of 6.5 km in length, right upstream of the reservoir, where the *rambla* enters a sinuous and narrow (~30e50 m in width) bedrock valley carved on Cretaceous limestones with alluvium at the valley bottom (Fig. 1). In this reach, sediments transported by the *rambla* are dominated by gravels and boulders, but a careful inspection of the valley sides revealed important accumulations of silt and sands deposited by high stage floodwaters. These slack-water flood deposits show a complete stratigraphy from which long-term flood records can be reconstructed.

A major challenge in the estimation of palaeoflood discharges in mixed bedrock-alluvial channels is assuming that the present valley geometry adequately represents the channel conditions at the time of flooding (Benito and O'Connor, 2013). In Rambla de la Viuda field inspection shows ubiquitous evidence of river channel incision, mainly since 1976 when in-stream gravel mining started (Calle et al., 2017). Former positions of alluvial surfaces can be identified by gravel lines and colour change marks on bedrock margins as well as by sharp horizontal boundaries on lichens size, which are indicative of different timing on rock exposure. The analysis of fluvial morphological changes over time was based on aerial photos (1946e2012) supported with LiDAR topography (year 2009) and GPS points taken on alluvial surfaces (Calle et al., 2017). A detailed incision map was obtained (Calle et al., 2017) showing the evidence of a pre-mining period (1946e1967) of undisturbed conditions, followed by the progressive degradation of the riverbed after 1967, indicating an average channel incision of 3.5 m. The uncertainty in flow boundary geometry requires specific consideration of the possible range of channel topography at the time of deposition of slackwater flood sediments.

3. Methodology

Quantitative palaeoflood methods were applied to reconstruct the magnitude and frequency of past floods using sedimentary evidence (Benito and O'Connor, 2013). The methodology follows two steps (1) documentation and description of slackwater flood deposits and other flood palaeostage indicators, and (2) relating the identified flood evidence (mainly flood depositional layers) to flood discharge based on hydraulic calculations. A detailed stratigraphy with emphasis on contacts between flood units was conducted at nine profiles. Individual flood units were identified through a variety of sedimentological indicators (Baker and Kochel, 1988; Benito et al., 2003a,b): the identification of clay layers at the top of a unit; erosion surfaces; bioturbation indicating the exposure of a sedimentary surface; angular clast layers, where slope materials were

deposited between flood events; and changes in sediment colour. As well as identifying individual flood units, sedimentary flow structures were also described in order to elucidate any changing dynamics during a particular flood event and/or infer flow velocities that can improve discharge estimation (Benito et al., 2015c). Flood units were sampled for geochemical and textural analysis and bio-minerals extractions. At selected sites, sediment peels of the stratigraphic profiles, measuring approximately 80 cm × 50 cm in size, were made in the field (Hattingh and Zawada, 1996; Thorndycraft et al., 2005).

Flood chronology was determined using radiocarbon and optically stimulated luminescence (OSL) ages collected from individual flood units. (Tables 1 and 2). Radiocarbon dating was carried out by the Accelerator Mass Spectrometry (AMS) technique in the facilities of the Department of Geography at the University of Zurich (GIUZ) and by Beta Analytics. For OSL dating, a total of ten sand samples were collected in the field using PVC cylinders, from which quartz grains were extracted for luminescence measurements avoiding exposure to daylight. The OSL dating (Aitken, 1998) was performed at the Nordic Laboratory for Luminescence Dating in Denmark.

The single aliquot regenerative dose (SAR) protocol (Murray and Wintle, 2000) was used for all measurements. Equivalent doses (D_e) were determined by interpolating the natural luminescence signal on the corresponding corrected dose response curve. Thermal transfer tests were undertaken on two of the 10 samples showing no significant effect of thermal transfer on the measured doses for preheat temperatures between 180 °C and 260 °C. Preheat temperature of 200 °C for 10 s and cut heat temperature of 180 °C, both at 5 °C/s have been used for all luminescence measurements unless otherwise stated. Approximately 2500e3000 single grains of size 180e250 mm from each of the 10 samples have been measured. Single grain OSL signals are derived from the summation of the first 0.1 s of stimulation corrected with the last 0.2 s for background (i.e. Late BackGround subtraction, LBG).

In order to compare the reproducibility of these results with those obtained using small aliquots, approximately 100 small aliquots were also measured for each sample. Multi-grain measurements were carried out using 2 mm aliquots containing ~30 grains each. The OSL signals from multigrain aliquots are based on the summation of the first 0.64 s of stimulation corrected for background using the following 0.64 s in order to eliminate the contribution of slow components (e.g. Early BackGround subtraction, EBG; Cunningham and Wallinga, 2010).

Several statistical approaches were used to estimate the burial dose and the derived age - arithmetic mean, the Central Age Model (CAM, Galbraith et al., 1999), the Minimum Age Model (CAM, Galbraith et al., 1999), and the Internal-External Consistency Criterion, (IEU, Thomsen et al., 2003, 2007). The exponential transformation suggested by Medialdea et al. (2014) has been applied prior to the use of CAM and MAM in cases which dose distribution contained negative and zero values. The IEU approach has been found to be the most suitable to determine the age of the samples studied here. A summary of the dated samples is presented in Table 2.

Cross-sections and flood deposit elevations, the input data for the hydraulic models, were surveyed along the study reach using a Trimble 4700 kinematic differential GPS. Channel geometry is the single most important factor in estimating flood discharge for a particular stage. As previously indicated, in our study reach channel incision has dominated since 1976 as result of in-stream gravel mining, requiring consideration of likely ranges of channel geometry at the time of flooding. The distribution of main fluvial landforms (active channel, active gravel bars, and vegetated gravel bars) was taken from the 1956 aerial photography considered as natural (pre-mining) channel morphology (1946e1967). The average elevation of the preserved gravel bar remnants identified in the 1956 mapping was linked to the landform at the specific cross-section (Fig. 2). These elevation data are consistent with the first topographic surveys on the stream bed performed by the Spanish Geographic Institute in 1938 (Municipality of Costur). The active channel width was measured on the aerial photographs and assumed to be inset ~1.5 m below the active gravel bar. The channel slope or difference on minimum channel elevation between cross-sections was assumed to be maintained equal to the thalweg surveyed in the field (RTK-GPS survey performed in 2011). Therefore, once we stablished the channel elevation at the most downstream cross-section under natural conditions, the minimum channel elevations in the upstream of cross-sections were calculated (Fig. 2). This assumption is corroborated by the slope of the longitudinal profile performed with remnants of gravel bars deposited under natural river conditions, and by the 1938 topographic survey.

The estimation of discharges associated with the elevations of slackwater flood deposits was carried out by computing the water surface profiles for various hypothetical discharges that were routed through the surveyed study reaches, and by comparing the model-generated profiles to the elevation of flood sediments. The hydraulic calculations were carried out through the step-backwater method (Webb and Jarrett, 2002) using the HEC-RAS software

Table 1
Radiocarbon ages were calibrated to calendar ages by using Oxcal 4.2 software (Bronk Ramsey, 2009) based on IntCal 13 Reimer et al. (2013) calibration data set. Some conventional 14C BP dates have multiple intercepts in the calendar year BP curve. Two Sigma calibrated age is provided in ranges with indication of their relative area (in %) under 2s distribution. The most likely age is an interpretation of the age range that best fit in relation to the stratigraphic context.

Flood unit	Sample material	Lab code	Age, 14C yrs BP	Calibrated age range (2s), yr BP	Calibrated age range, AD 95.4% probability	Most likely age range, AD
RVD2						
RVD2-12	Charcoal d13C: -40.0 ± 1.1‰	UZ-5713/ ETH-38307	335 ± 40	488-306 (95.4%)	1462-1644 (95.4%)	1460e1645
RVD2-6	Charcoal -24.9 ± 1.1‰	UZ-5714/ ETH-38308	220 ± 30	309-0 (95.4%)	1642-1684 (36.7%) 1735-1806 (44.7%) 1933e1945 (14.0%)	1640e1805
RVD5						
RVD5-10	Charcoal d13C: -25.7 ± 1.1‰	UZ-5712/ ETH-38306	160 ± 30	286-244 (16.7%) 231-124(47.4%) 118-66 (12.6%) 36-0 (18.6%)	1664-1706 (16.7%) 1719-1826 (47.4%) 1832e1884 (12.6%) 1914e1945 (18.6%)	1830e1945
RVD7						
RVD7-11	Charcoal	Beta-299036	100 ± 30	268-214 (27.1%) 145-15 (68.3%)	1682-1736 (27.1%) 1805e1935 (68.3%)	1805e1935

Table 2
Optically stimulated luminescence dating results from slackwater flood deposits in Rambla de la Viuda. OSL ages are estimated in years before the date of sampling. Last column of this table shows the ages converted to AD/BC to facilitate the comparison with the rest of ages reported in the manuscript. Quartz samples were extracted using routine lab procedures (Porat, 2006). Water contents were estimated at 2± 1%. a, b and g dose rates were calculated from the concentrations of the radioisotopes (K, U, Th) and the cosmic dose rates estimated from burial depths. D_e was determined using the single aliquot regeneration (SAR), with preheats of 10s @ 200e260C and test-dose preheats 20° lower. All samples show very good preheat plateaus, recycling ratios are mostly within 5% of 1.0 and IR recycling ratio within 2% of 1.0. No. of discs is the number from those measured that was used for calculating the D_e. Ages are in years before 2010, rounded to the nearest 5 or 10; errors rounded to the nearest 5 years.

Flood unit	Depth (cm)	Age (years b. 2010)			Equivalent dose (Gy)			Dose rate (Gy/ka)			Age AD/BC
RVD2-1	20	140	±	10	0.28	±	0.02	2.05	±	0.09	1860e1880
RVD2-5	100	240	±	20	0.39	±	0.02	1.59	±	0.07	1750e1790
RVD2-7	135	370	±	20	0.61	±	0.03	1.63	±	0.08	1620e1660
RVD5-2	50	110	±	10	0.19	±	0.01	1.79	±	0.08	1890e1910
RVD5-3	90	90	±	10	0.19	±	0.01	2.00	±	0.09	1910e1930
RVD5-5A	123	120	±	10	0.22	±	0.01	1.79	±	0.08	1880e1900
RVD5-5B	167	90	±	10	0.16	±	0.01	1.88	±	0.08	1910e1930
RVD8-8C	332	4580	±	240	8.48	±	0.18	1.85	±	0.08	2810e2330BC
RVD8-6	150	3840	±	210	7.67	±	0.17	1.99	±	0.09	2040e1620BC
RVD8-3	82	470	±	30	0.94	±	0.03	1.98	±	0.09	1510e1570

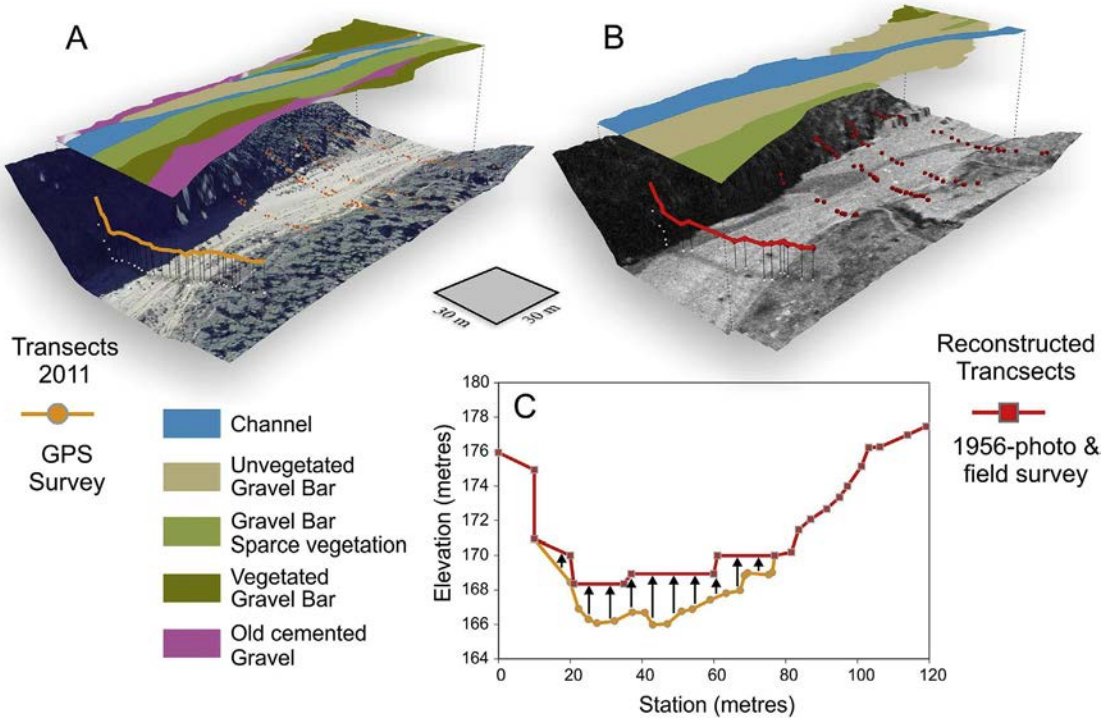

Fig. 2. Methodological approach for the reconstruction of valley bottom topography previous to in-stream gravel mining in operation since 1970s.

(Hydrologic Engineering Center, 2010). The computation procedure is based on the solution of the one-dimensional energy equation, derived from the Bernoulli equation, for steady gradually varied flow. Subcritical flow conditions were assumed along the reach, with critical flow selected as the boundary condition at the most downstream cross-section. Assigned Manning's n values were 0.03 for the valley floor and 0.04 for the margins. A sensitivity test performed on the model shows that for a 25% variation in the roughness values an error of 6e12% was introduced into the discharge results. These discharge estimates based on paleostage indicators represent a minimum discharge, and assuming slack-water deposition occur within a water depth of 1e1.5 m the estimated discharge may be close to real peak values.

Flood frequency analysis (FFA) was carried out on the annual flood series for the period 1959 to 2014 and the non-systematic record based on palaeoflood discharge estimates. The daily average discharges over the period 1959e2007 were transformed to peak discharges using the Fuller (1914) approach applied at regional level in the Júcar and SE-Ebro basins (CEDEX, 2011; a ¼ 37.73 and b ¼ 0.45). The frequency analysis was performed using the AFINS software (Botero and Francés, 2006). Flood record stationarity for censored samples (systematic and non-systematic) was checked using Lang's test (Lang et al., 1999). The 95% tolerance interval of the accumulated number of floods above a threshold, or censured level is computed. Stationary flood series are those remaining within the 95% tolerance interval (Naulet et al., 2005). A set of probability distribution functions was fitted to the flood data series and the parameters of these distribution functions were estimated by the maximum likelihood method (Stedinger and Cohn, 1986). The most robust results in terms of adjustment to the drawn plotting positions were obtained with a two-component extreme value (TCEV) distribution (Rossi et al., 1984).

Landuse and paleovegetation information along the alluvial and paleosol stratigraphic profiles was obtained from soils and

sediments geochemical analysis and from phytoliths analysis. Phytoliths were extracted from dry soil following the summarized protocol adapted from Kelly (1990). A total of 23 sediment samples, were weighted and prepared following the next summarized steps: a) dried; b) carbonate dissolution with HCl; c) reduction of iron oxides with trisodium citrate and sodium dithionite; d) oxidation of organic matter using H_2O_2 (30%); e) deflocculation in a sodium hexametaphosphate (5%) buffered at pH 7. A weighted part of the final AIC sediment was then placed in slides (76 × 26 mm) and mounted with Canada balsam. A Leica DM 2500P, with a digital camera Leica DFC 420C, was used for the phytoliths counting and other biominerals study.

Phytolith extraction from botanical samples followed the dry ashing methodology outlined by Parr et al. (2001). A total of 30 plant species were sampled, representative of the vegetation associations in the study area: *Quercus ilex* L, *Quercus cocciferae* L, *Pistacea lentiscus* L, *Olea europaea* L, *Ceratonia siliqua* L., *Prunus dulcis MILL*, *Pinus halepensis Mill*, *Pinus pinea* L, *Juniperus oxycedrus* L., *Cistus clusii Dunal*, *Rhamnus oleoides* L, *Coronilla minima* L, *Artemisia campestris* L, *Thymus vulgaris* L, *Rosmarinus officinalis* L, *Fumana thymofolia* L, *Festuca gautieri (Hack) K.Richt*, *Avena sterilis* L., *Panicum miliaceum* L, *Brachypodium retusum (Pers.) P.Beauv*., *Brachypodium phoenicoides* L, *Bromus diandrus Roth*, *Bromus hordaceus* L, *Bromus madritensis* L, *Juncus* sp, *Tamarix gallica* L, *Stipa tenacissima* L, *Carex acutiformis Ehrh*, *Arundo donax* L. Stem, leaf, Inflorescences and seeds were processed separately, and soil samples corresponding to main plant associations (evergreen sclerophylous maquis, traditional agroforestry systems, xerophytic vegetation abandon fields and pastures, overbank flooded areas) were also collected, processed and analyzed. The percentage of each morphotype per species was calculated and types were described according to the International Code for Phytolith Nomenclature (Madella et al., 2005).

Documentary flood data was compiled to complement the palaeoflood data. Archival flood evidence provides direct information of individual events (e.g. flood date, duration, stage or spatial extent) or indirect (e.g. post-flood damage repair) allowing flood chronologies and socio-economic impacts to be compiled (Brázdil et al., 2006; Benito et al., 2015c). The torrential and ephemeral characteristics of the Rambla de la Viuda have been historically a limiting factor for setting large human settlements near the *rambla*, and therefore, there is a lack of detail historical information on observed floods and their relative magnitude. A recent compilation of historical floods that occurred in the studied region was provided by Segura (2001, 2006) from scientific and technical reports, local history books and non-systematic compilations by historians (Cavanilles, 1795-1797; Balbás Cruz, 1892; Beltrán Manrique, 1958; Fontana Tarrats, 1978; Sánchez Adell et al., 1993). The available historical information of flooding in Castellón province dates back to the mid-1500s; however, the first flood reported for Rambla de la Viuda is the 1617 flood. The original documents were consulted and further investigated in order to provide a relative magnitude of each flood according to the damage description. In addition, we have carried out a search in newspaper archives for late 19th and 20th century floods, focussed on known flood dates. Such information was particularly valuable to establish the rank of flood damages and impact on the socio-economic activities.

4. Results

4.1. Historical and systematic flood records

Most of the available documentary floods were collected from local historical chronicles reporting damage in Castellón province (Table 3). In particular for the Rambla de la Viuda data is scarce and objectivity or continuity of the information is not guaranteed. It should be noted that flood perception by people living along the Rambla de la Viuda is perceived to be low, mainly because of absence of major settlements next to the river channel. Moreover, the lower reach of the *rambla* (region known as *La Plana*, The Plane) is deeply incised into Quaternary cemented alluvium and the overflowing on the old alluvial plain, where settlements are located, only occurs near the Mediterranean coast. Therefore, most of the reported floods are those producing important impacts on linear infrastructures crossing the *rambla* such as irrigation canals, roads and bridges.

In Rambla de la Viuda, six large flood events were reported over the period 1617e1900, namely in 1617, 1783, 1787, 1801, 1883, and 1900 (Table 3). These large floods documented for Rambla de la Viuda were also reported to affect the Millars River, including the gauged 20th century floods. It should be noted that before AD 1617, the historical flood record only refers to the Millars River (e.g. 1580, 1581, 1597; Beltrán Manrique, 1958), although it is very likely that these events also occurred in Rambla de la Viuda. More uncertain is the potential relation between floods in Rambla de la Viuda and floods reported in the Turia and Júcar rivers (at Valencia, ~75 km south; Ruiz et al., 2014). In this case, only the largest floods in the Turia river were also reported in Rambla de la Viuda (e.g. 1783, 1957, 2000).

Only one gauge station in the Rambla de la Viuda catchment (Vall d'Alba) is in operation since 2007 as part of the Automatic Hydrological Information Systems (SAIH) network. A longer record of daily discharge values (1956e2012) can be estimated from daily balance of water storage and release at the Maria Cristina Reservoir (construction started in 1910 and in operation since 1925). Detailed inspection of these daily discharges indicates an insufficient quality of the gauged discharge in particular for large floods. In addition, the daily water volumes at the reservoir show balance inconsistencies (e.g. negative values during low flow periods) that may be indicative of a low quality of the reservoir level readings. Since the construction of the Maria Cristina reservoir (1925), several large floods exceeded the spillway capacity (600 $m^3 s^{-1}$) overtopping the dam wall. Three incidents of dam overtopping were officially reported by the water authorities (1962, 1969 and 2000; Fig. 3A and B) and two cases of dam spillover occurred in 1920 and 1922 according to local newspapers (references in Table 3). The 1962-flood is the largest on record when the water overtopped the dam wall reaching a peak flow of 1500 $m^3 s^{-1}$, according to the dam manager (Mateu, 2011). The 1969-flood daily mean discharge was 238 $m^3 s^{-1}$ with an estimated peak flow of 585 $m^3 s^{-1}$ based on regional parameters of the Fuller equation. The 2000-flood peak flow was estimated in 1268 $m^3 s^{-1}$ (Gabaldó Sancho et al., 2002), although the recorded daily mean flow was 385 $m^3 s^{-1}$ giving a calculated peak of 945 $m^3 s^{-1}$ with Fuller's equation. Epigraphic marks at the dam wall show that flood stage during the 1969 flood was halfway between 1962-flood and 2000-flood levels, therefore it would agree with a more conservative peak flow (~945 $m^3 s^{-1}$) for the 2000-flood.

4.2. Palaeoflood hydrology

Along a 6.5 km study reach, a total of ten sites of slackwater deposition were described (Fig. 3C). Most of the sites correspond to flood deposit benches located at valley expansions and at backwater areas within tributary streams (Fig. 1). There are a number of flood evidences at high elevation rock shelters and within rock crevices containing remnants of laminated flood sediments but with poor stratigraphy.

The oldest flood sediments were recorded at site RVD8 located

Table 3
Chronology of the major floods in Rambla de la Viuda and assigned flood units in the stratigraphic profiles (number refers to stratigraphic profiles in Fig. 4). *Documentary flood not specifically reported for Rambla de la Viuda, although due to its regional extent is likely to affect the Viuda's catchment. Minimum discharges were estimated using sedimentary evidences as palaeostage indicator; the best estimate (reconstructed channel bed elevation in 1956 from aerial photo) is shown in bold characters. In same column, Qc and Qci corresponds to mean daily discharge and peak discharges from Maria Cristina Reservoir. The daily mean discharges over the period 1959e2007 were estimated from balance of input and output daily flow volumes in the Maria Cristina Reservoir. The daily values were transformed to peak discharges using the Fuller (1914) approach applied at regional level in the Júcar and SE-Ebro basins (CEDEX, 2011; a ¼ 37.73 and b ¼ 0.45). The last column shows the minimum discharge associated to palaeoflood units based on the calculations using the actual channel bed geometry.

Documentary record of large floods			Stratigraphic evidence		Flood discharge estimate	
Historical flood Date/ Most likely date	Comments	References	Flood unit in stratigraphic profile (Fig. 4)	Flood unit dating interval (years AD)	Minimum Q (m^3s^{-1}) Pre-incision channel bed elevation	Minimum Q (m^3s^{-1}) actual channel bed elevation
22 Oct - 3 Nov 1406*	Large floods in Jucar and Turia rivers.	Fogues, 1931; Fontana Tarrats, 1978; Ruiz et al., 2014				
25 Oct 1427*	Large floods in Jucar and Turia rivers.	Fogues, 1931; Fontana Tarrats, 1978; Ruiz et al., 2014	RVD2-14		700e800	1400
30 Nov 1473*	Large floods in Jucar rivers	Fogues, 1931; Fontana Tarrats, 1978	RVD2-12	C14: 1465 e1645	850e1100	1500e1700
Nov 1475*	Large floods in Crown of Aragon. Flood in Turia River	Fogues, 1931; Fontana Tarrats, 1978	RVD2-11		950e1200	1500e1700
27 Sept 1517*	One of the largest floods in Valencia region	Fontana Tarrats, 1978; Ruiz et al., 2014	RVD2-10 RVD8-3	OSL: 1510 e1570	1100e1400	1500e1700
16 Sept 1580*	Millars river, Sec river. Foods in Vila-real, Almassora and Borriana	Beltrán Manrique, 1958 Fontana Tarrats, 1978	e			
18 Sept 1581*	Millars river and Castellon region rivers. Destruction of Santa Quiteria bridge.	Beltrán Manrique, 1958 Fontana Tarrats, 1978	RVD2-8		1200e1500	2000e2400
9 Sept 1597*	Millars, Becaire and Sec rivers. Destruction of diques and canals	Beltran Manrique, 1958	e			
2 Nov 1617	Damage in a bridge in Rambla de la Viuda. Large floods in Valencia, Aragón and Catalonia	Segura 2001	RVD2-7 RVD8-2	OSL: 1620 e1660	1300e1600	2000e2400
24 Nov 1783	Flooding in R. de la Viuda. Several casualties in the region	Balbás Cruz 1892	RVD2-6	C14: 1640 e1805	1400e1700	2000e2400
8 Oct 1787	Large flood. Breakdown of the old Alcora Dam (built in ~1580) at Lucena river (tributary of R. de la Viuda).	Cavanilles, 1795-1797 Beltrán Manrique, 1958	RVD2-5	OSL: 1750 e1790	1500e1800	2000e2400
18 Nov 1801	Damages on buildings, roads and agricultural fields. Millars and other rivers in the region flooded	Beltrán Manrique, 1958; Sánchez Adell et al., 1993	RVD2-4	e	1550e1850	2000e2400
9 Oct 1883	Damage in roads, fields, mills and dams. Bridge in the road Castelló-Alcora destroyed. 43 casualties.	Balbás Cruz, 1892 Beltrán Manrique, 1958	RVD2-1 RVD8-1 RVD5-6 RVD7-9 gravel	OSL: 1860 e1880	1830e2200	2800
14 Sept 1900	Roads and villages flooded.	Segura, 2001 Newspaper Heraldo de Castellón	RVD5-5B RVD7-8	OSL: 1880 e1900	400e240	>500
21 Feb 1920	Flood affected the dam construction works. 1st overtopping of Maria Cristina dam	ABC newspaper 22.02.1920, p. 16	RVD5-5A RVD7-7	OSL: 1910 e1930	580e280 Qci > 560	>600 >800
15 Oct 1922	Most rivers in region flooded. In Mijares River Peak flow of 2898 m3s-1 2nd overtopping of Maria Cristina dam. Floodwater overtopping in 5 m the dam wall	ABC newspaper 18/10/1922, pp.19-20	RVD5-4 RVD7-6		600e300 Qci > 560	>600 >800
Mar 1946	Damage and erosion of the original spillway channel	Cordero Page et al., 2007 labyrinth spillway	RVD7-5		>300	>350
13e14 Oct 1957	27 10^6 m^3 reached the Maria Cristina reservoir	ABC 20.10.1957-p. 66	RVD7-4		>400 Qc:250 Qci:550	>450
16 Oct 1962	3rd overtopping of Maria Cristina dam	Cordero Page et al., 2007. ABC-17.10.1962-p.41; ABC SEVILLA-19.10.1962-p.1	RVD5-3 RVD7-3	OSL: 1910 e1930 Reverse dating	1630 Qc:660 Qci:1620	>650
5 Oct 1969	4th overtopping of Maria Cristina dam	Cordero Page et al., 2007 presa en laberinto	RVD5-2 RVD7-2	OSL: 1890 e1910 Reverse dating	650e450 Qc:238 Qci:585	~600
30 Dec 1989	Recorded in reservoir gauged data				>360	>400

Table 3 (*continued*)

Documentary record of large floods			Stratigraphic evidence		Flood discharge estimate	
Historical flood Date/ Most likely date	Comments	References	Flood unit in stratigraphic profile (Fig. 4)	Flood unit dating interval (years AD)	Minimum Q ($m^3 s^{-1}$) Pre-incision channel bed elevation	Minimum Q ($m^3 s^{-1}$) actual channel bed elevation
24 Oct 2000	5th overtopping of Maria Cristina dam. Real time gauge data not available.	ABC SEVILLA-25.10.2000, p. 10	RVD5-1 RVD7-1		Qc:285 Qci:700 900–720 Qc:385 Qci:945	>900
30 Sep 2009	Real-time gauge data (SAIH)				~200 Qc:65 Qci:153	

at a high bench within a valley expansion reach (Fig. 1). The stratigraphic profile is 4.7 m in thickness and shows two distinct sets (Fig. 4). The lower set overlays a gravel unit and it is composed of four units with fine to very fine sand and massive to slightly laminated structure. The most remarkable one is unit 8 which is ~2 m in thickness that most probably represents multiple flood events although there is a lack of discernible stratigraphic breaks. The base of unit 8 was OSL dated as 4580 ± 240 years whereas unit 6 at the top of the set was dated as 3840 ± 210 years (Table 2). This lower set is capped by a well developed soil with a lag of colluvial boulders and gravels. The upper set overlying the soil comprises at least five flood units characterised by fine to very fine sand with dominant parallel lamination. At the middle of this set, unit 3 was OSL dated as 470 ± 30 years (AD 1510–1570; most likely age AD 1517), therefore recording one of the largest floods on the documentary record. Hydraulic computations of flood flow within the reach using HEC-RAS model indicates that the lower set units are associated with a discharge range 360–800 $m^3 s^{-1}$, whereas the upper most recent (last 600 years) flood set corresponds with a minimum discharge between 800 and 1200 $m^3 s^{-1}$ (Fig. 4), the latter within the upper rank of the current flood magnitudes.

Profile RVD2 is located at the mouth of a tributary stream that joins the canyon on the right side forming a re-entrant that is inundated during large floods (Fig. 3E). At this site, a 3.5-m thick SWD sequence is composed of cohesive sands interrupted at the mid-section by a gravel unit with source in the tributary stream and at the upper section by two colluvial units composed by sand and scattered gravels (4 mm) and pebbles (Fig. 4). At the bottom, there are at least four flood units (units 10, 11, 12 and 14) underlying tributary alluvial gravel; the second lowest one (unit 12) was radiocarbon dated as 335 ± 40 ^{14}C years BP (cal. AD 1460–1645 at 95.4% probability). A soil (colour 10YR6/4) was developed on this unit 12 characterised by coarse blocky structure oriented clay skins or cutans (7.5YR5/5), indicating an environmental stability phase under prevailing wet conditions. A second edaphic phase, longer than the previous one, affected units 10 and 11, although the soil (10YR6/6) is less developed than the previous one. These flood units were deposited by flows exceeding 700 $m^3 s^{-1}$. The ~1 m-thick mid-section tributary gravelly unit consists of at least three sets: the lower composed by angular poorly sorted stratified and imbricated medium to coarse gravel; the middle on clear erosive contact composed by very angular poorly sorted and disorganised cobble to boulder gravel; and the upper of angular sorted stratified medium to fine gravel supported on a sand matrix (Fig. 4). Overlying the tributary gravel, the stratigraphy shows at least six flood units composed by very fine sands with parallel lamination, with upper contacts with frequent root and bioturbation marks. The estimated age indicates that this flood deposition took place during the 17th and 18th centuries by discharges larger than ~1200 $m^3 s^{-1}$ (Fig. 4). Since the 17th century there is evidence of scarce environmental stability reflected on the lack of well-developed soils, notably since unit 7 which includes a 15–20-cm thick soil horizon (7.5YR6/4). The upper stratigraphic section is dominated by two colluvial units of ~30 cm thick each, with sand and granule textures with crude flat bedding typical of slope washout flow facies, indicating a long period with lack of flood deposition at this site. The uppermost flood unit is ~40 cm thick and consists of fine to very fine sand with well developed parallel and ripple lamination. This flood event was OSL dated as 140 ± 10 years (AD 1860–1880), and it is the highest depositional evidence of a flood along the studied reach with a minimum discharge of 1830 $m^3 s^{-1}$ (Fig. 4).

The most recent flood deposits are represented in profiles RVD7 and RVD5. Profile RVD5 is located at a canyon expansion reach (Figs. 1 and 3F), corresponding to a lower flood bench (highest point at 6 m above channel) inset on the high-standing flood terrace (RVD8). The discharge estimations associated to this flood bench showed minimum discharges of 200–900 $m^3 s^{-1}$ (Fig. 4), therefore recording moderate magnitude flooding (deposition at low elevation). This lower flood bench accumulated a 3.4 m thick sequence with evidence of at least nine flood units composed of fine and very fine sand with clear contacts between units. The bottom units (8, 9 and 10), consist of fine to very fine sands with diffuse parallel lamination, the lowest one was radiocarbon dated as of 160 ± 30 ^{14}C yrs BP (cal AD 1830–1945). Overlying this lower flood set, there was accumulated a 25 cm-thick colluvial unit composed of pebble gravels and sands most likely reworked from former fluvial material. The upper flood set contains at least six depositional events, the lowest three (units 4–6) contain parallel lamination and scattered ripples with diffuse contacts between units indicative of short time span between floods; units 1–3 include climbing ripples in-drift, at the base of the sequence, followed by parallel lamination with clear contacts by bioturbation and root marks (Fig. 4). Unit 5 is ~70 cm in thickness with a lack of stratigraphic breaks although a close inspection shows an incipient Bt soil horizon at 30 cm from the base. The OSL dating provided reversal ages of 90 ± 10 (base) and 120 ± 10 (top) years (Table 2) most likely deposited at beginning of the 20th century. This is also suggested by a piece of aluminium foil embedded at the top of unit 2. This unit was deposited by discharges over 650 $m^3 s^{-1}$, suggesting that units 2 and 1 were most likely deposited by the 1989 and 2000 floods.

Profile RVD7 is located ~1 km downstream of RVD5 at a canyon expansion where a flood bench was accumulated on the right valley margin (Fig. 1). The flood bench is 2.5 m in thickness and contains at least ten flood units. The oldest flood unit was dated as 100 ± 30 ^{14}C years BP (cal. AD1805–1935) indicating a temporal framework similar to RDV5. Overlying the lowest two flood units, a gravelly

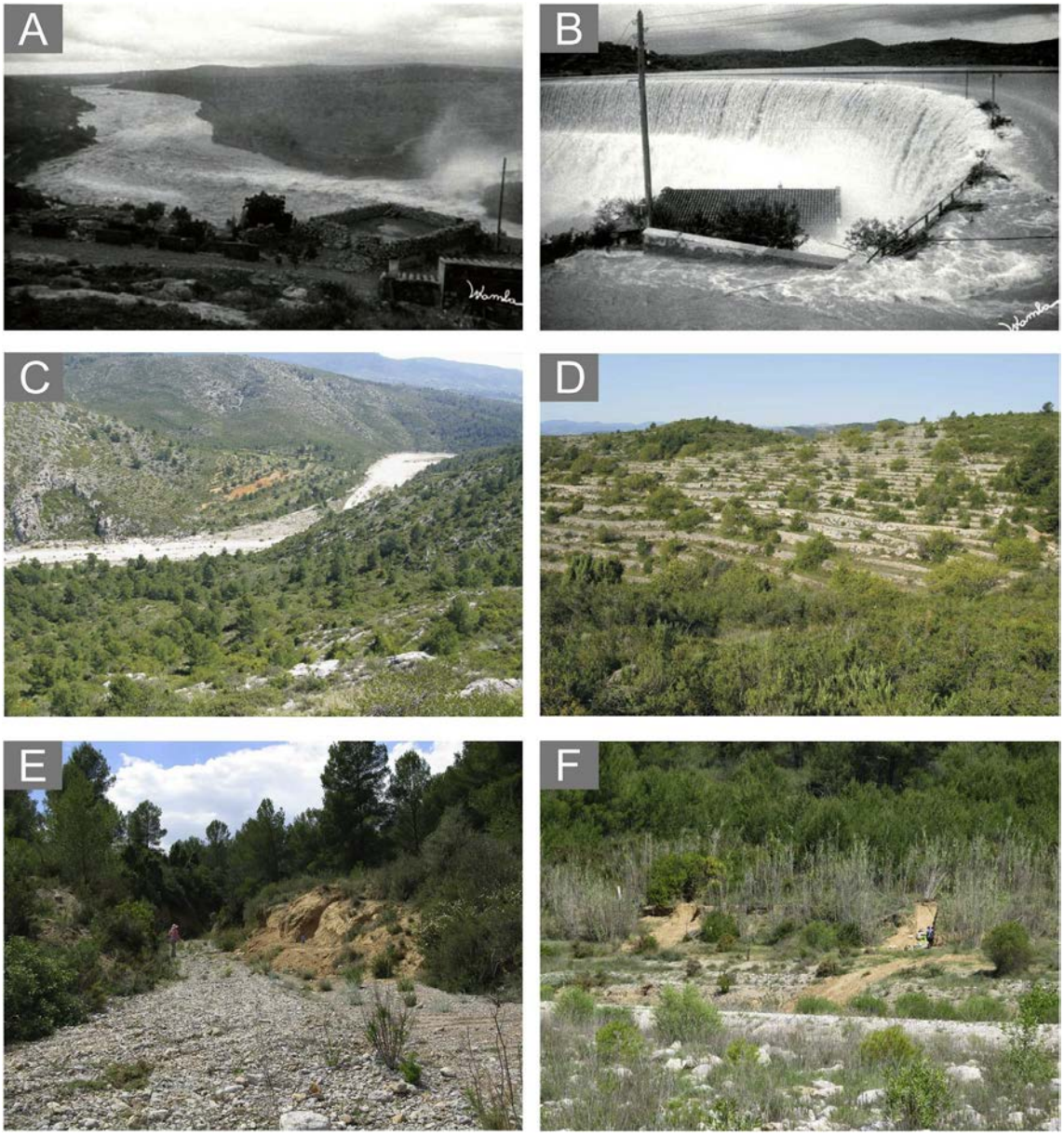

Fig. 3. A: Rambla de la Viuda downstream of María Cristina dam during the 1962-flood. B: Flood waters overtopping the Maria Cristina dam upto 1.7 m in depth during the 1962-flood. C: General view of the middle reach river valley entrenched on limestones and marls of Cretaceous age, as well as Pliocene and Pleistocene conglomerates and sandstones. D: Agricultural terracing built during the 19th to early 20th century and currently abandoned and occupied by shrubs and pine trees. Land-use changes during historical times have modified soil infiltration properties and therefore runoff and sediment yield during extreme rainfall. E: Slackwater flood deposits site RVD2 located upstream of a tributary junction. F: Slackwater flood deposits bench on an expansion reach, and view of a clean face dug for description of stratigraphic profile RVD5. Note standing people for scale.

colluvial unit was accumulated which resembles in position and facies the one described in RVD5. The upper stratigraphic set consists of eight flood units composed of fine to very fine sand with clear contacts between units. Their sedimentary sequence includes parallel lamination, cross-bedding structures, ripple marks, and climbing ripples in-drift with reverse flow direction indicative of eddy flow at this site. These SWDs at an elevation of 4 m over the stream channel provided a minimum discharge of 150e720 $m^3 s^{-1}$ (Fig. 4).

4.3. Historical vegetation dynamics

Present day vegetation in the Rambla de la Viuda basin consists of remnants of a mosaic of an evergreen sclerophyllous maquis (*Quercus cocciferae* L., *Pistacea lentiscus* L), a long-established traditional agroforestry system in upper stream mountain areas (*Quercus Ilex*, *Olea europaea* L, *Ceratonia siliqua* L., *Prunus dulcis* MILL, *Pistacea lentiscus* L, *Pinus pinea* L) and the prevailing presence of thorny xerophitic vegetation (herbaceous and shrubs) together with patches of partly reforested areas (*Pinus halepensis* L) in carbonaceous rock outcrop areas (Fig. 2D). The xerophitic herbaceous and shrub vegetation cover most of the watershed area and occupy communal grazing areas as well as old cultivated scattered areas. Along the overbank flooding areas, vegetation communities include *Brachypodium retusum (Pers.) P.Beauv.*, *Brachypodium phoenicoides* L, *Bromus diandrus Roth*, *Bromus hordaceus* L, *Bromus madritensis* L, *Juncus* sp, *Tamarix gallica* L, *Stipa tenacissima* L, *Carex acutiformis Ehrh*, *Arundo donax* L.

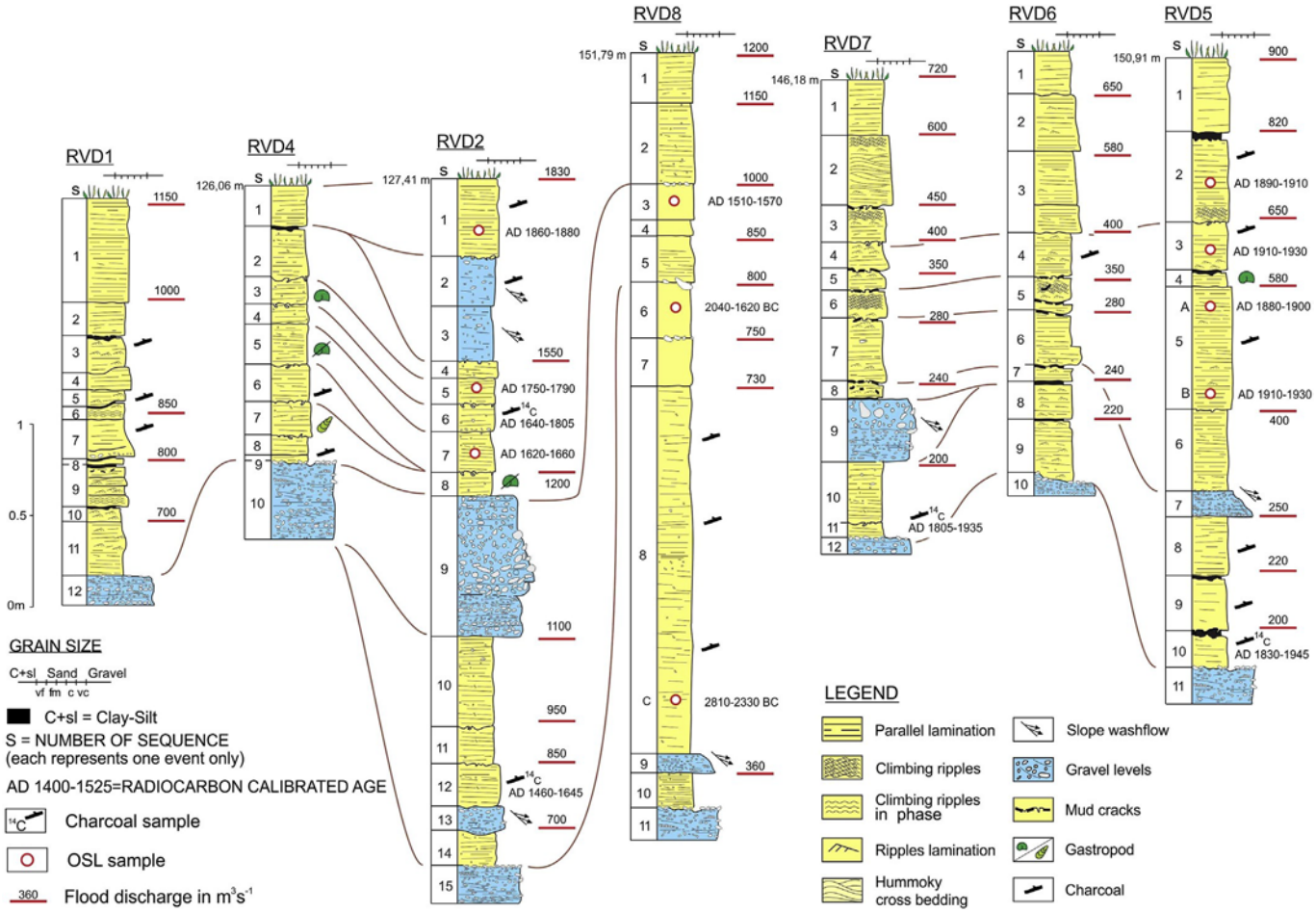

Fig. 4. Stratigraphic profiles at the study reach (radiocarbon dates in calibrated years AD) and proposed correlations between sections.

The historical land cover variations associated with periods of greater hydroclimatic variations in the study area periods was reconstructed using the phytholith content in the sediments sampled at the different stratigraphic units. The sediments, both colluvial and fluvial, have a poor organic matter content (0.1e2.1%), a high pH (8.4e9.4) and often poor phytoliths content which could be related not only to the production of silica opal phytoliths by xerophytic vegetation, but to their preservation and dissolution in high energy and alkaline environments (Piperno, 2006; Fraysse et al., 2009). Phytolith extraction from the sediments collected along the different sedimentary units of the stratigraphic profiles RVD2 and RVD5 have nevertheless yielded a statistically significant bioliths count for most of the sampled units. Sediments sampled at the upper sequence of RVD7 and RVD6 also yielded a significant bioliths count, covering the last 100 years stratigraphic record. The fine sediments (silt fraction) sampled at the stratigraphic units corresponding to high energy transport fluvial bars deposits were found to be sterile in all sampled profiles. Overall, higher phytolith count is associated with the presence of edaphic activity and its preservation in uneven. Samples collected at lower stratigraphic profile units, fluvial or colluvial, are less well preserved (weathering, erosive) than the bioliths extracted from the upper stratigraphic units. Geochemical analyses indicate low contents on O.M., N, K and Al, even in horizons with higher phytoliths content, which can be related not only to the lithological characteristics of the watershed substratum, but to excessive carbonate content.

Overall, from the species analyzed, only 13 (*Quercus* sp, *Pinus* sp., *Juniperus oxycedrus* L., *Pistacia lentiscus* L., *Rosmarinus officinalis* L., *Artemisia campestris* L, *Olea* sp., *Tamarix gallica* L, *Juncus* sp., *Cistus* sp, *Carex acutiformis* Ehrh, *Arundo donax* L) were found to produce uniquely shaped phytoliths: crenate type in the case of Quercus sp, polyhedral with bordered pit impressions and honeycomb in conifers (except in the case of the *Juniperus oxycedrus* L), and cuneiform, tabular scrobiculated, trapeziform sinuate and long saddle in the ligneous diagnostic species of the xerophytic and overbank areas. Although species on degraded grazing areas, both low slope areas and in overbank flood areas (Other/Riparian in Figs. 5 and 6), produced a large number of non-diagnostic morphologies and types, modern soil samples associated to these areas indicate a high percentage of three phytolith morphologies pattern: elongated acicular, elongated parallepiped and trapeziform short cells.

Profile RVD2 records the sedimentary register of the oldest preserved palaeoflood deposits in the study area (since 15th century). All sedimentary units, colluvial and fluvial were sampled and three had a very low count (<50 counting's per sample) and these results were not plotted in Fig. 5. The phytoliths analysis indicate a high concentration of grass-produced phytoliths throughout the sedimentary sequence, which suggest that herbaceous formation have been a significant part of the study area vegetation through historical times. Edaphic activity which resulted in the formation of the six buried palaeosols identified in this profile, affecting fluvial (lower units) or colluvial (two most recent palaeosols) deposits, is related to a strong component of herbaceous cover. The better developed soils, (affecting units 10, 11 and 12) indicate a higher

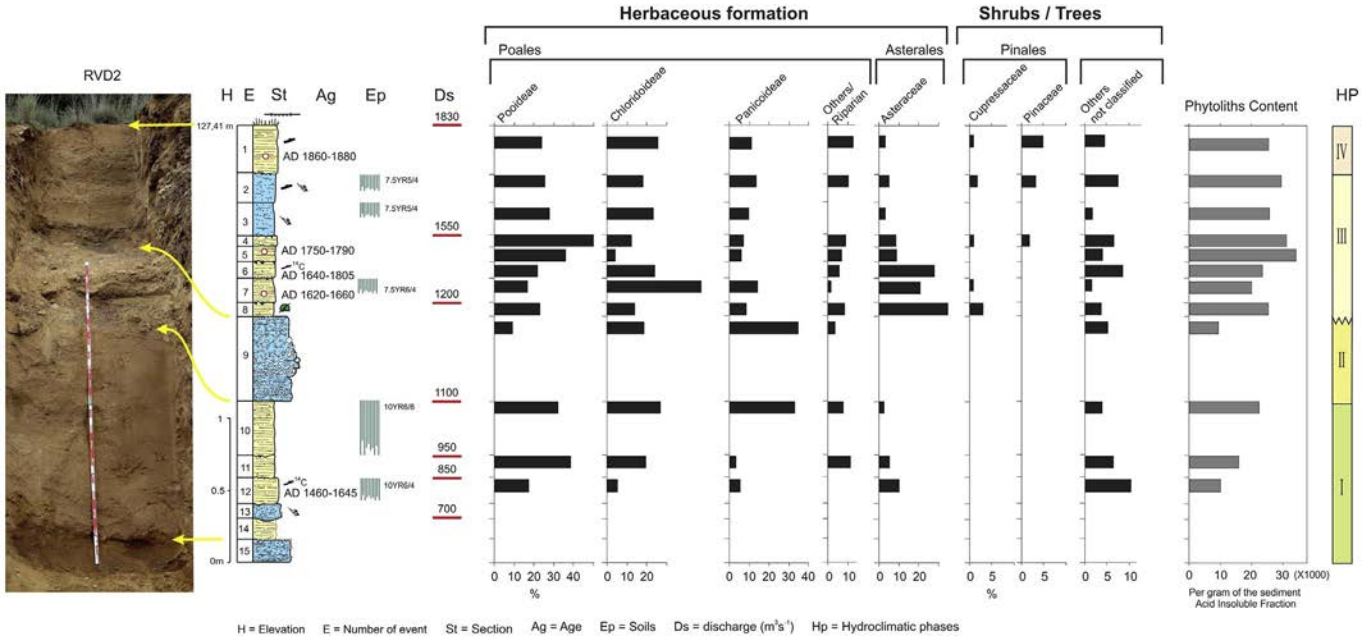

Fig. 5. Stratigraphic profile RVD2 composed of slackwater flood deposits units intercalated with slope and tributary fluvial gravelly deposits and vegetation changes derived from phytolith content analysis. The column on the right indicates the hydroclimatic phases occurring over the last 500 years.

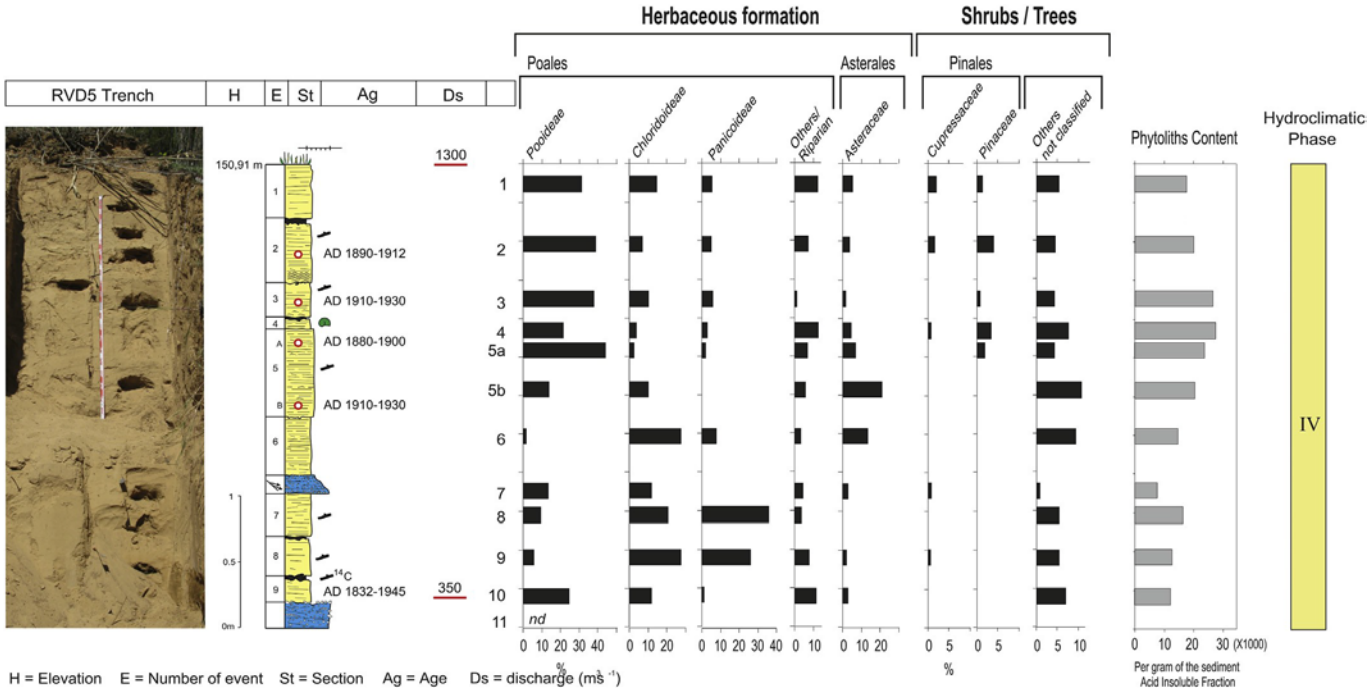

Fig. 6. Stratigraphic profile RVD5 composed of slackwater flood deposits units deposited since late 19th century and phytolith content indicative of vegetation changes.

presence of C_3 type herbaceous species (*Avena* sp, *Bromus* sp), which decrease their presence towards the top of the sequence, and in a less extent of morphologies from the *Asteraceae* and *Cupressaceae* groups. Multicellular polyhedral morphology type combining tetra and pentahedral cells of *Ceratonia silicua* L were found in unit 12 (RVD2-12). The lowest fossil bioliths count is found in RVD2-9, corresponding to a sediment sample collected at the top of a tributary alluvial deposit (presenting synsedimentary edaphic activity). The sedimentary unit deposited at the top of this alluvial deposit (RVD2-8) indicates a clear increase on C_3 herbaceous species as well as of pasture/riparian species and woody plants. Samples collected at RVD2-7, corresponding to a slope washout flow sedimentary facies, mark a sharp shift from previous soil water content conditions (high presence of C_3 herbaceous coverage and increasing woody presence). Analysis reveals not only a decrease on fossil bioliths count but the marked increase of C_4 species and less than 5% of riparian vegetation and woody species. Geochemical analysis of the sediments that have a slope longitudinal

contribution, indicate an increase in total N content, which is not related to an increase on the OM content (0.34%) nor to the presence of fossil micro or macroplants. Although tentative, an increase on C_4 (*Chloridoideae*) plants, which in the study area largely correspond to herbaceous coverage on degraded carbonaceous areas and grazing pastoral drylands, could suggest not only a period of soil water stress conditions but the abandoning of cultivated lands and increase of grazing activities. Towards the top of the sedimentary sequence, there is a moderate increase of herbaceous cover of the C_4 *Panicoideae* morphotypes and *Asteraceae* type, and a sharp increase on C_3 morphotypes in units RVD2-5 and 6 (late 18th century). The maximum herbaceous morphotypes count were yielded at RVD2-4. Regarding woody plants morphotypes, there is a reduction on *Cupressaceae* types and morphotypes related to *Pinus* sp were identified for the first time in this sedimentary sequence. The samples collected at RVD2-3 and 2, corresponding to two buried poor developed soils over distal fan deposits, indicate a retreat on *Asteraceae* type morphotypes. Woody species morphotypes are poorly represented on RDV2-3 and increase their presence again (*Pinaceae*) toward the end of the profile, which yielded a radiocarbon dating from the end of the 19th century.

Profile RVD5 (Fig. 6) comprises the better preserved and continuous record of the sedimentary registry that took place in the study area since late 19th century till the present day. The lower units of the stratigraphic profile (10-8) corresponding to the intercalation of fluvial deposits, with signs of herbaceous roots and dry mud cracking at surface, with slope lateral transport and very superficial rework. An incipient A/C buried paleosol was developed over sedimentary unit 10. The three flood sets are limited at bottom and top of the sequence by thick colluvial deposits. This sedimentary assemblage yielded the poorest phytoliths count, and is characterised by a predominance of C_4 (*Chloridoideae* and *Panicoideae*) morphology types. Phytolith analyses of the sediments of unit RVD5-6 indicate a clear shift from the previous evidences of low soil water availability and landscape degradation. There is a progressive change, in the herbaceous species composition, from C_4 to C_3 type predominance towards the top of the stratigraphic profile, as well as an increase on the woody species morphologies. *Pinaceae* related morphologies were retrieved from upper sedimentary units (5-1) dating from the end of the 19th century. The best developed buried soil along the current profile affects the unit RVD5-5 where two Bt horizons can be identified, which indicates a discontinuity on the sedimentation. The coarse blocky structure and oriented clay skins may indicate that phytoliths translocation could have happened. Two samples were taken (5A, 5B). Although no important changes on the *Poales* composition were observed, RDV5-5B presents an important content on *Asteraceae* types: turnover or surface exposition and two different units. This would explain the dating reversal results provided by the OSL chronology in unit 5A and 5B (Fig. 4, Table 2).

4.4. Flood frequency analysis

The incorporation of palaeoflood data in the FFA raises the problem of stationarity of flood series, which is one of the basic assumptions of the frequency analysis. Among the main potential factors affecting stationarity of flood series are land-use changes and climate variability. Historical environmental changes based on bio-indicators are likely to affect runoff during minor and moderate rainfalls. However, the largest floods require soil saturated conditions which seems more independent of land-use and vegetation cover. Stationary tests (Lang et al., 1999) of the combined palaeoflood and instrumental flood series above 1000 $m^3 s^{-1}$ show stationary conditions over the period 1617e2014.

Palaeoflood information is considered data censored above

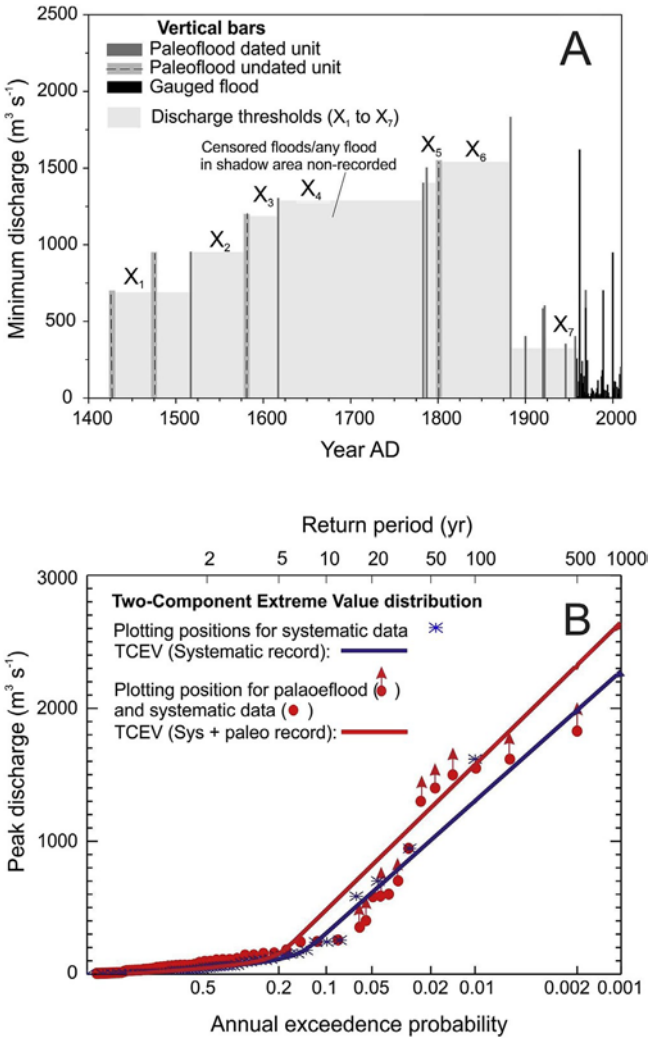

Fig. 7. A: Organisation of palaeoflood data and systematic annual floods for flood frequency analysis. B: Two component extreme value (TCEV) distribution fitted with (1) systematic data and (2) systematic and historical flood data. Dots represent the plotting positions for the systematic record (blue dots) and palaeoflood plus systematic records (red dots). (For interpretation of the references to colour in this figure legend, the reader is referred to the web version of this article.)

threshold (Fig. 7A). Hence, it is assumed that the number of k floods exceeding an arbitrary discharge threshold (X_T) in M years is known, similar to partial-duration series (Stedinger and Cohn, 1986; Francés et al., 1994). Palaeoflood data are organised according to different fixed threshold levels over particular periods of time exceeded by flood waters. In reality, there are self-rising discharge thresholds since the deposition of a sand-silt layer accreting at the flood bench raises the minimum water stage required to leave the next one (Fig. 7A). Moreover, the exceedance probabilities of floods represented on the sediment pile decrease as layers are built up. The value of the peak discharge for the palaeofloods above X_T may be known or unknown.

The flood frequency distribution providing the best performance in the combination of non-systematic (censured) and systematic data was the Two Component Extreme Value (TCEV) distribution function. Discharge values associated to different exceedance annual probabilities (recurrence intervals) with the TCEV distribution function is shown in Table 4. The visual matching and the statistical parameters indicate that the distribution fitting is good (Fig. 7B; Table 4). The use of palaeoflood data in the frequency

Table 4
Flood quantiles for different return periods in Rambla de la Viuda for a two-component extreme value (TCEV) distribution fitted to, firstly, the annual maximum systematic records only and secondly, to the combined systematic and censored palaeoflood discharges.

Exceedence annual probability (%)	Average recurrence interval years	Discharge Syst.þ paleofloods [m^3 s^{-1}]	Discharge (Systematic Record) [m^3 s^{-1}]
20	5	155	110
10	10	480	305
4	25	920	710
2	50	1250	1000
1	100	1570	1300
0.2	500	2305	1975
0.1	1000	2615	2250

analysis results in higher values of magnitude of the flood quantiles than those obtained with only the systematic record (Table 4). For instance, the 1% annual probability flood based on combined palaeoflood and instrumental datasets is 1570 m^3 s^{-1} whereas using only the systematic record is 1300 m^3 s^{-1}. Moreover, the 1000-yr flood conventionally used for hydraulic design of dam spillways resulting from our frequency analysis is 2615 m^3 s^{-1}, which highlights the deficient design of the current dam spillway (600 m^3 s^{-1}) evidence by the frequent dam overtopping which represents an important risk for dam safety of the Maria Cristina dam.

5. Discussion

5.1. Interpreting the record of the largest floods

Rambla de la Viuda contains multiple stratigraphic and geomorphic evidence of extreme flooding from which to reconstruct a detailed history of the largest floods. Along the study reach, flood evidences include gravel and boulder bars, drift-wood, erosion marks, and occasionally fine-texture slack-water flood deposits. Slackwater deposits in the Rambla de la Viuda gorge are preserved in two distinct depositional environments, namely at flood benches in canyon expansion reaches (Fig. 3F), and at tributary mouths (Fig. 3E). Slackwater flood benches have been described in different palaeoflood studies as preferred source of flood stratigraphy (Kochel et al., 1982; Benito et al., 2003a). These flood benches are developed by standing or slow-moving water which allows a better preservation of flood deposits through time, particularly on those ones protected from destruction by flows on the main stem (e.g. profiles RVD2 and RVD8). Flood deposits occupying valley margins next to the high flow channel are expected to be periodically removed by very extreme floods and replaced by sediments left by smaller magnitude floods. These episodic erosion flood processes can explain the short term flood history within profiles RVD5 and RVD7, whose stratigraphic record was likely reset by the 1883 flood, the most extreme flood in Rambla de la Viuda over the last 500 years.

The hydrology of Rambla de la Viuda is dominated by flash floods, therefore reconstructing the long-term pattern of flooding enables understanding the hydrological and sedimentological processes involved in the evolution of this ephemeral stream. As in other ephemeral gravel bed streams in semiarid Mediterranean environments, Rambla de la Viuda generates contrasting perceptions among local population: as a potential source of water for agriculture but also as a source of hazards by damaging events. For instance the stone bridge that crosses the *rambla* in Almanssora was destroyed and built several times since the 15th century (Arciniega, 2015) affecting the trade not only among villages but between Barcelona and Valencia. Perception of those water resource vs hazards issues could change through time according to the prevailing hydroclimatic conditions, associated to flood rich and flood poor periods occurring at multidecadal scales.

The lack of a continuous and homogeneous historical flood data from Rambla de la Viuda can be attributed to the limited number of villages and population settled next to the water course, a direct consequence of its lack of sustainable water resources and its deadly torrential flows. Only during the last century, since the construction of the Maria Cristina reservoir, news of flooding from Rambla de la Viuda became relevant because of the risk of dam failure associated to dam overtopping during the 20th Century major floods. However, the major historical floods reported in local chronicles since early 17th century are in high agreement with the palaeoflood archive both in terms of the number and chronology of floods (Table 3). In other words, the palaeoflood chronology was validated by historical flood archives, under the assumption that all major documentary floods were potentially recorded in the flood stratigraphy, and periods with a lack of historical floods were frequently reflected in the stratigraphy by accumulation of colluvium and tributary sediments.

The earliest palaeoflood sediments in Rambla de la Viuda were deposited about 4600 years ago (Table 2) but it terms of continuous stratigraphy, the palaeoflood record provides a 600-year interval of frequency and magnitude of the largest floods. Fig. 7A shows a combined historical-palaeoflood record; vertical dark bars representing OSL and radiocarbon dated flood units and vertical grey lines correspond to undated stratigraphic units that were assigned to dates of known historical floods that occurred within the interval of the dated units. Ten large floods took place between AD 1400 and 1900 (recorded in profiles RVD2 and RVD8) with the largest one reaching a minimum discharge of 1830 m^3 s^{-1}. Initially, only floods with discharge exceeding 700 m^3 s^{-1} were included in the record and, as successive flood layers were accumulated, this threshold of discharge was increased resulting in progressive longer elapsed time intervals between flood units. The average time interval between floods is ~45 years, although eventually either some of these large floods occurred after 2e4 years since the previous one, or after a long period of ca 170 years without major floods (e.g. 1618e1783; Segura, 2001). In the Turia River, a period of low flood frequency was also reported between 1620 and 1770, with the exception of 1671e1695 (Ruiz et al., 2014). The later decrease in frequency is attributed to the rise in minimum discharge (1200 m^3 s^{-1}) required to leave a flood layer in the flood bench (RVD2 above unit 7 in Fig. 4). The absence of very large floods during that period was corroborated by the lack of reported floods in the documentary record. The flood series shows an acceptable stationarity along the palaeoflood record, with only one period recording a minor flood cluster in 20 years at the end of the 18th Century (1783, 1787, 1801). This flood cluster coincides climatically with the "Maldà Anomaly" (1760e1800) described for the Western Mediterranean as a period of high hydrological variability (floods and droughts, Barriendos and Llasat, 2003). The post-Maldà stratigraphic record was dominated by the accumulation of slope

deposits, which coincides with the absence of reported floods in the historical documents (Table 3).

The most catastrophic flood event in terms of magnitude and impacts corresponded to the October 9th, 1883 flood, which according to the palaeoflood evidence reached a minimum discharge of 1830 $m^3 s^{-1}$, exceeding the largest flood recorded during the 20th century (1500 $m^3 s^{-1}$). According to local newspapers the damage was extreme with destruction of four bridges in the road Castellón to Lucena (with five arcs), the Alcora's bridge, the Faya's bridge and Figuerola's bridge (El siglo Futuro, 15/10/1883). The flood caused at least 43 casualties, several bodies were found along the Mediterranean coast. The slackwater flood accumulation of this 1883-flood (OSL dated) was found at top of RVD2 profile, comprising fine sand with parallel lamination being remarkable in its 40 cm in thickness, twice that of previous deposited layers. The high sediment volume associated to this extreme event is indicative of the duration and sediment load carried during the flood.

The October 8th 1787 flood was also reported as a major event that caused the break of the Alcora dam built in 1580 according to chronicles by Cavanilles in 1795e1797 (Perez Medina, 2002). According to the stratigraphy, this flood could have exceeded 1500 $m^3 s^{-1}$, being of a similar order of magnitude to the 1783 and 1801 floods. The November 2nd, 1617 flood is the largest documented flood in many rivers and ephemeral streams in NE Spain, and documents refer to this episode as the deluge year (Thorndycraft et al., 2006). The stratigraphic evidence of this flood was assigned to unit 7 in profile RVD2 ($Q > 1200$ $m^3 s^{-1}$) being the thickest one over the time interval 1550e1810, followed by a flood-poor period represented by colluvium and gully deposition (Fig. 5).

During the 20th century, at least three floods exceeded 1000 $m^3 s^{-1}$ which were recorded at profiles RVD5 and RVD7, although none of them exceeded the discharge of the 1883 flood in RVD2 (1830 $m^3 s^{-1}$). The lower bench (RVD5 and RVD7) contains evidence of at least eight palaeofloods over the last 125 years with a minimum discharge of 200e900 $m^3 s^{-1}$. Radiocarbon and OSL chronologies were not conclusive in providing accurate flood dates, except on the fact all there were deposited since late 19th, most likely following the catastrophic 1883-flood. The palaeoflood layers have been assigned to documentary flooding in official reports, newspapers articles, and gauged data. The gauge data (1956e2014) were estimated from the daily balance of water storage and release at the Maria Cristina Reservoir. This daily mean discharge was used to calculate the peak flows assuming a regional correlation between mean daily discharge and peak discharge obtained from multiple gauge station records (CEDEX, 2011, Table 3). The largest gauged flood occurred on October 15, 1962 when the water overtopped the dam wall reaching according to the dam manager logbook record a peak flow of 1500 $m^3 s^{-1}$. Water authorities reported other events of water overflowing its embankment dam beyond its spillway capacity (600 $m^3 s^{-1}$) in 1920, 1969 and 2000. In addition, newspaper reports indicate that dam overtopping also occurred in 1922. Flood peak flows are unknown except for the 2000-flood estimated in 1268 $m^3 s^{-1}$ (Gabaldón Sancho et al., 2002) although flood marks at a pillar standing on the dam indicates an intermediate flood discharge between the 1962 and 1969 floods (likely ~945 $m^3 s^{-1}$).

In terms of the large floods, their frequency has been maintained and even decreased slightly towards one large flood every 30e40 years. Floods in Rambla de la Viuda over the 20th century were similar in magnitude to those recorded during the 15th, 16th and 17th centuries. However, the largest floods in the 18th and 19th century recorded ca 25% higher peak flows than current ones (Fig. 7A). The effects of climate (increasing dryness) and/or land-use change affecting runoff volume, peak discharge and frequency may explain the higher torrential hydrological regime (Millan et al., 1995). In fact, other Iberian Mediterranean rivers, such as the Guadalentin river, increased their flood magnitudes and energy conditions over the 18th and 19th centuries coinciding with historical evidence of major economic and land-use changes (major deforestation and increase in cultivated land into marginal areas; Benito et al., 2008, 2010).

A flood magnitude similar to the 1883-flood could pose a serious risk of collapse to the current Maria Cristina reservoir that in case of failure could bring catastrophic consequences to the Vila-Real and Almanssora communities. Currently, there is a plan to increase the spillway capacity to support a design flood of 3154 $m^3 s^{-1}$ (flood with average recurrence interval of 1000 years) and to increase the dam maximum flood upto 5620 $m^3 s^{-1}$ (10,000-year flood). According to our palaeoflood study, the 1000-year flood corresponds to 2615 $m^3 s^{-1}$, similar to the projected design flood, although the safety check flood (10,000-yr flood) gives a peak flood of 3565 $m^3 s^{-1}$.

5.2. *Environmental history and climatic context*

The environmental proxy indictors, namely phytolith content, soils and geochemical content, combined with the hydroclimatic indicators (palaeoflood and documentary records) identifies four hydro-climatic phases (Fig. 8).

Over the 15th to 16th centuries (Phase I), a high frequency and magnitude of floods occurred in relation with two periods of relative increase in wetness at cal. AD 1450e1475 and AD 1550e1620. In this phase, minimum estimated discharges of the largest floods ranged between 700 and 1300 $m^3 s^{-1}$. Phase II (17th to mid-18th century) is characterised by absence of large magnitude flooding ($Q > 1000$ $m^3 s^{-1}$). In the stratigraphy, the scarce SWD units (Q: 350e1000 $m^3 s^{-1}$) are intercalated with colluvial deposits. The analysis of phytoliths indicates a predominance of herbaceous species of C4 photosynthetic pathway, with less than 5% of riparian vegetation and woody species. The content of phytoliths during this period of maximum aridity was 5×10^3 units per gram of sediment (acid-insoluble fraction). In comparison, the mean phytolith content in the Phase I sediment samples is 40×10^3 units per gram.

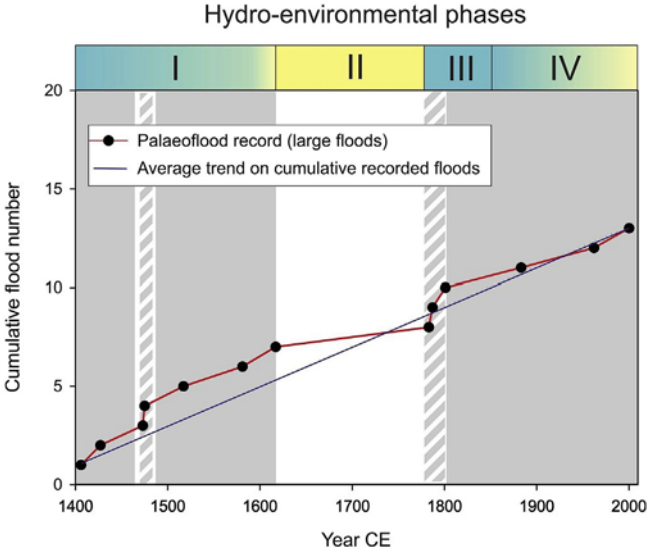

Fig. 8. (a) Accumulated number of palaeoflood events recorded since AD 1400. Shaded areas show the temporal distribution of flood clusters described in the text. Above, phases of homogeneous environmental conditions derived from evidence from the stratigraphic palaeoflood record, soil development, paleovegetation (phytolith content) and geochemical indicators.

This phase II is likely representing a high hydrological variability (frequent droughts punctuated with heavy rainfalls and flooding) and in general, with dry conditions, as it can be interpreted from the analysis of phytolith content in fluvial and colluvial deposits. Phase III from the end of the 18th century to middle 19th century, shows wetter conditions than the preceding period. During this period, which includes the Maldà Anomaly (Barriendos and Llasat, 2003), three major floods occurred in 1783, 1787 and 1801, exceeding 1400 $m^3 s^{-1}$. Phase IV spans from middle 19th century to present time, showing a progressive aridity since mid-20th century. Sedimentary records contain at least 10 flood events since 1880's to 1940's, with minimum flows estimated between 400 and 1830 $m^3 s^{-1}$, and the development of two paleosols. These edaphic stages are however less developed than those found in Phase I. This lower edaphic development is interpreted as due to greater climate and environmental instability during the last 100 years (Machado et al., 2011). In the last 50 years, there have been two major floods, one in 1962 and another in 2000, with estimated flows of 1500 and 945 $m^3 s^{-1}$, respectively. These flows are lower than those produced at the end of the 18th and beginning of the 19th century, when the agricultural and cattle pressure had its peak. The flood episodes recorded in Rambla de la Viuda during the Little Ice Age, largely agree in time with three documentary flood periods along the Mediterranean Spanish coastal area (1570e1630, 1760e1800 and 1830e1870; Barriendos and Martin-Vide, 1998). Similar flood periods were also reported for the historical record of the largest floods in the Turia and Jucar Rivers (Ruiz et al., 2014), and Guadalentin-Segura rivers (Machado et al., 2011).

6. Conclusions

This paper presents a 600-yr flood record of extreme events in Rambla de la Viuda, one of the largest ephemeral rivers in eastern Spain, based on stratigraphic descriptions of slackwater flood deposits and soils at seven sites supported by age dating (^{14}C and OSL methods) and sediment sampling for paleovegetation, chemical and textural analysis. The climatic and environmental conditions at the time of flooding were interpreted from the analysis of bioindicators, namely phytolith, and geochemical content. The estimation of palaeoflood discharges associated to the slackwater flood units was problematic due to evidence of an average river channel incision of 3.5 m since 1967, when in-stream gravel mining activities started. Flow boundary geometry prior to the gravel mining was reconstructed based on geomorphic mapping from historical aerial photography (1946e1967) and the topographic survey of preserved gravel bars currently perched on the valley margins. The channel slope or difference on minimum channel elevation between cross-sections was assumed to be equal to the present topography.

The palaeoflood record covers the last 4500 years, although complete stratigraphic evidence of the largest floods is available for the last 600 years. The average flood occurrence of large floods (>1000 $m^3 s^{-1}$) is of one event every 40 years as recorded at 1420e1620 and 1883 to the present. Decrease in occurrence of large floods during 1620e1775 (absence of large floods) coincides with the Late Maunder Minimum (1675e1715 AD) of decreasing solar activity with cold and dryer conditions in eastern Spain. A short period of higher frequency of large floods at 1775 to 1810 (at least three large floods) coincide with wetter conditions of decadal duration that coincides climatically with the Maldà Anomaly. The largest flood on record corresponds to the 1883-flood that produced catastrophic impact on Rambla de la Viuda.

Combined palaeoflood, palaeovegetation and geochemical proxies provide an environmental history of the climatic and land-use context of the catchment at the time of flood. Four phases with different palaeoflood frequency and magnitude were identified since the early 15th century.

Phase I (15th to 16th centuries): Highest flood magnitude records with minimum flood estimated discharges between 700 $m^3 s^{-1}$ and 1300 $m^3 s^{-1}$. It correlates in time with general wetter conditions (higher presence of C_3 photosynthetic pathway grasses and significant trees/bushes coverage. Two well-developed paleosols identified corresponding to wetter than normal periods ca 1550e1620 AD and 1670e1700 AD) preceding periods of palaeoflood sedimentary sequences.

Phase II (17th to mid-18th century): Lowest flood magnitude discharges and frequency for the 500 years sedimentary record. Estimated minimum discharges between 350 and 1000 $m^3 s^{-1}$. Flood sequences were interrupted by colluvial events. Sedimentological and phytolithic analysis of the fluvial and colluvial sediments indicate drier climatic conditions - low bioliths content in general, high presence of C_4 plants and the presence of less than 5% of riparian and dicots. Historical documents mention drier than usual conditions during middle 18th century.

Phase III (late 18th to early-19th century): Environmental conditions were wetter than the preceding period with three major floods (1783, 1787, 1801), exceeding 1400 $m^3 s^{-1}$. Phytolithic content indicates a progressive change, in the herbaceous species composition, from C_4 to C_3 type predominance towards the end of Phase III as well as an increase on the woody species morphologies (*Pinaceae*).

Phase IV (mid-19th entury to present): High frequency of floods (at least 10 events) since 1880's to 1940's, with the largest peak occurring in 1883 (1830 $m^3 s^{-1}$). During the last 50 years two large floods have occurred, in 1962 and 2000, with estimated discharges of 1500 and 945 $m^3 s^{-1}$. Since early 20th century, the phytolithic content shows a relative increase on C_4 herbaceous coverage which is more efficient in terms water use and adapted to warmer conditions in degraded carbonaceous areas.

The long-term behaviour of high magnitude floods (>1000 $m^3 s^{-1}$) has been stationary over the last 500 years. However, moderate-to-low magnitude floods over the last 150 years shows a trend towards a decreasing frequency, which correlates with other Mediterranean basins hydrological patterns during the 20th and early years of 21st century (Benito et al., 2008, 2010). The flood frequency analysis using instrumental record and palaeoflood discharge estimates shows flooding able to fulfill the spillway discharge capacity occurs with an average return interval of 30 years. Dam overtopping poses a serious risk to the safety of Maria Cristina dam, which would require an increase on the spillway flow capacity from its current de 600 $m^3 s^{-1}$ up to 2615 $m^3 s^{-1}$ matching the average 1000-yr flood considering the floods recorded over the last 500 years (the largest one exceeding 1830 $m^3 s^{-1}$).

Acknowledgments

This study was funded by the Spanish Ministry of Economy and Competitiveness through the research projects FLOOD-MED (ref. CGL2008-06474-C02-01), and CLARIES (ref. CGL2011-29176), by the CSIC PIE Intramural Project (ref. 200430E595), and by Fundación Biodiversidad (MAPAMA) through research project DAMadapt.

References

Aitken, M.J., 1998. An Introduction to Optical Dating. Oxford University Press, Oxford, 267 pp.

Arciniega, L., 2015. Puentes de cantería en el Reino de Valencia de la Edad Moderna: construcción y polisemia. Lexicon 20, 21e34.

Baker, V.R., 1987. Paleoflood hydrology and extreme flood events. J. Hydrol. 96, 79e99.

Baker, V.R., 2008. Paleoflood hydrology: origin, progress, prospects. Geomorphology

101 (1e2), 1e13.
Baker, V.R., Kochel, R.C., 1988. Flood sedimentation in bedrock fluvial systems. In: Baker, V.R., Kochel, R.C., Patton, P.C. (Eds.), Flood Geomorphology. John Wiley & Sons Ltd., USA, pp. 123e137.
Balbás Cruz, J.A., 1892. El libro de la provincial de Castellón. Imprenta y librería de J. Armengot, Castellón. 872 pp.
Barriendos, M., Llasat, M.C., 2003. The case of the 'Maldà' anomaly in the western Mediterranean Basin (AD 1760-1800): an example of a strong climatic variability. Clim. Change 61, 191e216.
Barriendos, M., Martín Vide, J., 1998. Secular climatic oscillations as indicated by catastrophic floods in the Spanish Mediterranean coastal area (14th-19th centuries). Clim. Change 38, 473e491.
Beltrán Manrique, E., 1958. Almanzora. El Mijares. Narración Histórica. Castellón. Armengot, 458 pp.
Benito, G., Brázdil, R., Herget, J., Machado, M.J., 2015a. Quantitative historical hydrology in Europe. Hydrol. Earth Syst. Sci. 19, 3517e3539.
Benito, G., Macklin, M.G., Panin, A., Rossato, S., Fontana, A., Jones, A.F., Machado, M.J., Matlakhova, E., Mozzi, P., Zielhofer, C., 2015b. Recurring flood distribution patterns related to short-term Holocene climatic variability. Sci. Rep. 5, 16398. http://dx.doi.org/10.1038/srep16398.
Benito, G., Macklin, M.G., Zielhofer, C., Jones, A., Machado, M.J., 2015c. Holocene flooding and climate change in the Mediterranean. Catena 130, 13e33. http://dx.doi.org/10.1016/j.catena.2014.11.014.
Benito, G., O'Connor, J.E., 2013. Quantitative paleoflood hydrology. In: Shroder, John F., Wolh, E. (Eds.), Treatise on Geomorphology, vol. 9. Academic Press, San Diego, pp. 459e474.
Benito, G., Rico, M., Sánchez-Moya, Y., Sopeña, A., Thorndycraft, V.R., Barriendos, M., 2010. The impact of late Holocene climatic variability and land use change on the flood hydrology of the Guadalentín River, southeast Spain. Glob. Planet. Change 70, 53e63.
Benito, G., Thorndycraft, V.R., Rico, M.T., Sánchez-Moya, Y., Sopeña, A., Botero, B.A., Machado, M.J., Davis, M., Pérez-González, A., 2011. Hydrological response of a dryland ephemeral river to southern African climatic variability during the last millennium. Quat. Res. 75, 471e482.
Benito, G., Sánchez-Moya, Y., Sopeña, A., 2003a. Sedimentology of high-stage flood deposits of the Tagus River, Central Spain. Sedimen. Geol. 157, 107e132.
Benito, G., Sopeña, A., Sánchez, Y., Machado, M.J., Pérez-González, A., 2003b. Palaeoflood record of the Tagus river (Central Spain) during the late Pleistocene and Holocene. Quat. Sci. Rev. 22, 1737e1756.
Benito, G., Thorndycraft, V.R., Rico, M., Sánchez-Moya, Y., Sopeña, A., 2008. Palaeoflood and floodplain records from Spain: evidence for long-term climate variability and environmental changes. Geomorphology 101, 68e77.
Botero, B.A., Francés, F., 2006. AFINS Version 2.0-Análisis de Frecuencia de Extremos con Información Sistemática y No Sistemática. Research Group on Hydraulic and Hydrology. Department of Hydraulic Engineering and Environment, Politechnical University of Valencia. http://lluvia.dihma.upv.es/.
Brázdil, R., Kundzewicz, Z.W., Benito, G., 2006. Historical hydrology for studying flood risk in Europe. Hydrol. Sci. J 51 (5), 739e764.
Bronk Ramsey, C., 2009. Bayesian analysis of radiocarbon dates. Radiocarbon 51 (1), 337e360.
Calle, M., Alho, P., Benito, G., 2017. Channel dynamics and geomorphic resilience in an ephemeral Mediterranean river affected by gravel mining. Geomorphology 285, 333e346.
Camarasa, A.M., Segura, F., 2001. Flood events in Mediterranean ephemeral streams (ramblas) in Valencia region. Spain. Catena 45, 229e249.
Cavanilles, A. J., 1795-97. Observaciones sobre la Historia Natural, Geografía del Reyno de Valencia. Imprenta Real, Madrid, 2 vols. Reproducción Facsímil, Ediciones Albatros, Valencia, 1985, 2 vols.
CEDEX, 2011. Mapa de Caudales Máximos. Memoria Técnica, Madrid, 67 pp.
Cordero Page, D., Elviro Garcia, V., Granell Ninot, C., 2007. Aliviaderos en laberinto. Presa de María Cristina. Ingen. Civ. 146, 15e18.
Cunningham, A., Wallinga, J., 2010. Selection of integration time intervals for quartz OSL decay curves. Quat. Geochronol. 5, 657e666.
Dahan, O., Tatarsky, B., Enzel, Y., Kulls, C., Seely, M., Benito, G., 2008. Dynamics of flood water infiltration and ground water recharge in hyperarid desert. Ground Water 46 (3), 450e461.
Ely, L.L., Enzel, Y., Baker, V.R., Cayan, D.R., 1993. A 5000-year record of extreme floods and climate change in the southwestern United States. Science 262, 410e412.
Fogués, F., 1931. Las inundaciones de la Ribera. An. del Cent. Cult. Valencia. IV (10), 232e250.
Fontana Tarrats, J.M., 1978. Historia del clima en el litoral mediterráneo: Reino de Valencia más Provincia de Murcia unedited, 206 pp.
Francés, F., Salas, J.D., Boes, D.C., 1994. Flood frequency analysis with systematic and historical or palaeoflood data based on the two-parameter general extreme value modes. Water Resour. Res. 30, 1653e1664.
Fraysse, F., Pokrovsky, O.S., Schott, J., Meunier, J.D., 2009. Surface chemistry and reactivity of plant phytoliths in aqueous solutions. Chem. Geol. 253, 197e206. http://dx.doi.org/10.1016/j.chemgeo.2008.10.003.
Friedman, J., Lee, V., 2002. Extreme floods, channel change, and riparian forests along ephemeral streams. Ecol. Monogr. 72 (3), 409e425.
Fuller, W.E., 1914. Flood flows. Trans. Am. Soc. Civ. Eng. 77, 564e617.
Gabaldó Sancho, O., Fleitz, J., Villalba Bergado, F., 2002. SAIH Flood warning system and emergency management in the Júcar basin (Spain): the case study of October 2000. In: Mitigation of Climate Induced Natural Hazards (MITCH) Workshop II: Advances in Flood Forecasting, P. 15, Barcelona (Spain), 10-12 June 2002. Flood Warning and Emergency Management.
Galbraith, R.F., Roberts, R.G., Laslett, G.M., Yoshida, H., Olley, J.M., 1999. Optical dating of single and multiple grains of quartz from Jinmium rock shelter, Northern Australia: Part 1, experimental design and statistical models. Archaeometry 41, 339e364.
Greenbaum, N., Schick, A.P., Baker, V.R., 2000. The palaeoflood record of a hyperarid catchment, Nahal Zin, Negev Desert, Israel. Earth Surf. Process. Landf. 25, 951e971.
Greenbaum, N., Schwartz, U., Benito, G., Porat, N., Cloete, G.C., Enzel, Y., 2014. Paleohydrology of extraordinary floods along the Swakop river, Namib desert and paleoclimate implications. Quaternary science reviews. Quat. Sci. Rev. 103, 153e169.
Gregory, K.J., Benito, G., Dikau, R., Golosov, V., Johnstone, E.C., Jones, J.A.A., Macklin, M.G., Parsons, A.J., Passmore, D.G., Poesen, J., Soja, R., Starkel, L., Thorndycraft, V.R., Walling, D.E., 2006. Past hydrological events and global change. Hydrol. Process 20, 199e204.
Grodek, T., Benito, G., Botero, B.A., Jacoby, Y., Porat, N., Haviv, I., Cloete, G., Enzel, Y., 2013. The last millennium largest floods in the hyperarid Kuiseb River basin, Namib Desert. J. Quat. Sci. 28, 258e270.
Hattingh, J., Zawada, P.K., 1996. Relief peels in the study of palaeoflood slack-water sediments. Geomorphology 16, 121e126.
Huang, C.C., Pang, J., Zha, X., Su, H., Jia, Y., 2011. Extraordinary floods related to the climatic event at 4200 a BP on the Qishuihe River, middle reaches of the Yellow River, China. Quat. Sci. Rev. 30, 460e468.
Hydrologic Engineering Center, 2010. HEC-RAS, River Analysis System, Hydraulics Version 4.1. Reference Manual, (CPD-69). US, Army Corps of Engineers, Davis, 411 pp. http://www.hec.usace.army.mil/software/hec-ras/hecras-document.html.
Kale, V., 2007. Fluvio-sedimentary response of the monsoon-fed indian rivers to late pleistocene-holocene changes in monsoon dynamics: reconstruction based on existing 14C database. Quat. Sci. Rev. 26 (11e12), 1610e1620.
Kelly, E.F., 1990. Methods for Extracting Opal Phytoliths from Soil and Plant Material. Internal Report. Department of Agronomy, Colorado State University, Fort Collins, 10 pp.
Knox, J.C., 1983. Responses of river systems to Holocene climates. In: Wright Jr., H.E. (Ed.), Late-quaternary Environments of the United States, V2. Univ. of Minnesota Press, Minneapolis, pp. 26e41.
Kochel, R.C., Baker, V.R., Patton, P.C., 1982. Paleohydrology of southwestern Texas. Water Resour. Res. 18, 1165e1183.
Kundzewicz, Z.W., Kanae, S., Seneviratne, S.I., Handmer, J., Nicholls, N., Peduzzi, P., Mechler, R., Bouwer, L.M., Arnell, N., Mach, K., Muir-Wood, R., Brakenridge, G.R., Kron, W., Honda, Y., Benito, G., Takahashi, K., Sherstyukov, B., 2013. Flood risk and climate change-global and regional perspectives. Hydrol. Sci. J. 59 (1), 1e28.
Lang, M., Ouarda, T.B.M.J., Bobée, B., 1999. Towards operational guidelines for over-threshold modeling. J. Hydrol. 225, 103e117.
Llasat, M.C., Puigcerver, M., 1990. Cold air pools over Europe. Meteorol. Atmos. Phys. 42, 171e177.
López-Bermúdez, F., Conesa-García, C., Alonso-Sarría, F., 2002. Floods: magnitude and frequency in ephemeral streams of the Spanish Mediterranean region. In: Bull, L.J., Kirkby, M.J. (Eds.), Hydrology and Geomorphology of Semi-arid Channels. John Wiley & Sons, Chichester, England, pp. 329e350.
López Gómez, A., 1987. Els Embassaments Valencians Antics. Generalitat Valenciana. Spain, 72 pp.
Machado, M.J., Benito, G., Barriendos, M., Rodrigo, F.S., 2011. 500 years of rainfall variability and extreme hydrological events in Southeastern Spain drylands. J. Arid. Environ. 75, 1244e1253. http://dx.doi.org/10.1016/j.jaridenv.2011.02.002.
Macklin, M.G., Fuller, I.C., Jones, A.F., Bebbington, M., 2012. New Zealand and UK Holocene flooding demonstrates interhemispheric climate asynchrony. Geology 40, 775e778.
Madella, M., Alexandre, A., Ball, T., 2005. International Code for phytolith nomenclature 1.0. Ann. Bot. 96, 253e260.
Mateu, J.F., 2011. La Primera Confederación Hidrográfica del Júcar (1934-1942). Confederación Hidrográfica del Júcar. Valencia. 156 pp.
Mateu, J.F., 1974. La Rambla de la Viuda. Clima e hidrología. Cuad. Geogr 15, 47e68.
Mateu, J.F., 1975. Sedimentología de la Rambla de la Viuda. Cuad. Geogr 16, 65e90.
Mateu, J.F., 1988. Crecidas e inundaciones en el País Valenciano. Guia de la Naturaleza de la Comunidad Valenciana. Edicions Alfons el Magnànim, Diputación Provincial de Valencia, pp. 595e636.
Medialdea, A., Thomsen, K.J., Murray, A.S., Benito, G., 2014. Reliability of equivalent-dose determination and age-models in the OSL dating of historical and modern palaeoflood sediments. Quat. Geochronol. 22, 11e24.
Millán, M., Estrela, M., Caselles, V., 1995. Torrential precipitations on the Spanish east coast: the role of the Mediterranean sea surface temperature. Atmos. Res. 36, 1e16.
Morin, E., Grodek, T., Dahan, O., Benito, G., Kulls, C., Jacoby, Y., Van Langenhove, G., Seely, M., Enzel, Y., 2009. Flood routing and alluvial aquifer recharge along the ephemeral arid Kuiseb River, Namibia. J. Hydrol. 368, 262e275.
Murray, A.S., Wintle, A.G., 2000. Luminescence dating of quartz using an improved single-aliquot regenerative-dose protocol. Radiat. Meas. 32, 57e73.
Naulet, R., Lang, M., Ouarda, T.B.M.J., Coeur, D., Bobée, B., Recking, A., Moussay, D., 2005. Flood frequency analysis of the Ardèche River using French documentary sources from the last two centuries. J. Hydrol. 313, 58e78.
Parr, J.F., Lentfer, C.J., Boyd, W.E., 2001. A comparative analysis of wet and dry ashing

techniques for the extraction of phytoliths from plant material. J. Archaeol. Sci. 28, 875e886.
Pèrez Medina, T., 2002. Petits embassaments Valencians del Segle XVIII. Cuad. Geogr 71, 11e30.
Piperno, D.R., 2006. Phytoliths: a Comprehensive Guide for Archaeologists and Paleoecologists. AltaMira Press, Lanham, Maryland, 238 pp.
Porat, N., 2006. Use of magnetic separation for purifying quartz for luminescence dating. Anc. TL 24, 33e36.
Reimer, P.J., Bard, E., Bayliss, A., Beck, J.W., Blackwell, P.G., Bronk Ramsey, C., Grootes, P.M., Guilderson, T.P., Haflidason, H., Hajdas, I., Hattz, C., Heaton, T.J., Hoffmann, D.L., Hogg, A.G., Hughen, K.A., Kaiser, K.F., Kromer, B., Manning, S.W., Niu, M., Reimer, R.W., Richards, D.A., Scott, E.M., Southon, J.R., Staff, R.A., Turney, C.S.M., van der Plicht, J., 2013. IntCal13 and Marine13 radiocarbon age calibration curves 0-50,000 years cal BP. Radiocarbon 55 (4), 1869e1887.
Rodríguez-Lloveras, X., Bussi, G., Francès, F., Rodríguez-Caballero, E., Solè-Benet, A., Calle, M., Benito, G., 2015. Patterns of runoff and sediment production in response to land-use changes in an ungauged Mediterranean catchment. J. Hydrol. 531, 1054e1066.
Rossi, F., Fiorentino, M., Versace, P., 1984. Two-component extreme value distribution for flood frequency analysis. Water reour. Res. 20 (6), 847e856.
Ruiz, J.M., Carmona, P., Pèrez Cueva, A., 2014. Flood frequency and seasonality of the Jucar and Turia Mediterranean rivers (Spain) during the "Little Ice age". Mèditerranèe 122, 121e130. http://dx.doi.org/10.4000/mediterranee.7208.
Sànchez Adell, J., Olcina Montis, F., Sànchez Almela, E., 1993. Elenco de fechas para la historia urbana de Castellòn de la Plana. Soc. Castellonense de Cultura. Castellòn, 215 pp.
Shannon, J., Richardson, R., Thornes, J., 2002. Modelling event-based fluxes in ephemeral streams. In: Bull, L.J., Kirkby, M.J. (Eds.), Dryland Rivers Hydrology and Geomorphology of Semi-arid Channels. John Wiley & Sons, Chichester, England, pp. 129e172.
Schick, A.P., 1988. Hydrologic aspects of floods in extreme arid environments. In: Baker, V.R., Kochel, R.C., Patton, P.C. (Eds.), Flood Geomorphology. Wiley Interscience, New York, pp. 189e203.
Segura, F., 2001. Evolución urbana e inundaciones en Castellò. Cuad. Geogr 69e70, 253e278.
Segura, F.S., Camarasa, A., 1996. Balances hídricos de crecidas em ramblas mediterraneas: Pèrdidas hídricas. In: Marzol, M.V., Dorta, P., Valladares, P. (Eds.), Clima y agua: la gestiòn de un recurso climàtico. La Laguna University, Tenerife, pp. 235e245.
Segura, F.S., 1990. Las Ramblas Valencianas. PhD Thesis. Universitat de València, 229 pp.
Segura, F.S., 2006. Las inundaciones de la Plana de Castellò. Cuad. Geogr 79, 75e100.
Simòn, J.L., Pèrez-Cueva, A.J., Calvo-Cases, A., 2013. Tectonic beheading of fluvial valleys in the Maestrat grabens (eastern Spain): insights into slip rates of Pleistocene extensional faults. Tectonophysics 593, 73e84.
Stedinger, J.R., Cohn, T.A., 1986. Flood frequency analysis with historical and Paleoflood information. Water Resour. Res. 22, 785e793.
Thomsen, K.J., Jain, M., Bøtter-Jensen, L., Murray, A.S., Jungner, H., 2003. Variation with depth of dose distributions in single grains of quartz extracted from an irradiated concrete block. Radiat. Meas. 37, 315e321.
Thomsen, K.J., Murray, A.S., Bøtter-Jensen, L., Kinahan, J., 2007. Determination of burial dose in incompletely bleached fluvial samples using single grains of quartz. Radiat. Meas. 42 (3), 370e379.
Thorndycraft, V.R., Benito, G., 2006. The Holocene fluvial chronology of Spain: evidence from a newly compiled radiocarbon database. Quat. Sci. Rev. 25, 223e234.
Thorndycraft, V.R., Barriendos, M., Benito, G., Rico, M.T., Casas, A., 2006. The catastrophic floods of A.D.1617 in Catalonia (NE Spain) and their climatic context. Hydrol. Sci. J. 51 (5), 899e912.
Thorndycraft, V.R., Benito, G., Rico, M., Sopeña, A., Sànchez, Y., Casas, M., 2005. A long-term flood discharge record derived from slackwater flood deposits of the Llobregat River, NE Spain. J. Hydrol. 313 (1e2), 16e31.
Thornes, J., Lòpez-Bermúdez, F., Woodward, J., 2009. Hydrology, river regimes, and sediment yield. In: Physical Geography of the Mediterranean. Oxford University Press, Woodward, J, pp. 229e253.
Webb, R.H., Jarrett, R.D., 2002. One-dimensional estimation techniques for discharges of paleofloods and historical floods. In: House, P.K., Webb, R.H., Baker, V.R., Levish, D.R. (Eds.), Ancient Floods, Modern Hazards: Principles and Applications of Paleoflood Hydrology. Water Science and Application Series, vol. 5. American Geophysical Union, Washington, DC, pp. 111e125.
Zawada, P.K., 2000. Palaeoflood hydrological analysis of selected south african rivers. Memoir of the council for geoscience, South Africa. Memoir 87, 173pp.
Zhang, Y., Huang, C.C., Pang, J., Zha, X., Zhou, Y., Gu, H., 2013. Holocene paleofloods related to climatic events in the upper reaches of the Hanjiang River valley, middle Yangtze River basin, China. Geomorphology 195, 1e12.